J. exp. Biol. 147, 53–89 (1989)
Printed in Great Britain © The Company of Biologists Limited 1989

STRUCTURE AND MECHANICS OF STARFISH BODY WALL

BY PATRICIA O'NEILL*

Department of Zoology, Duke University, Durham, NC, USA

Accepted 11 July 1989

Summary

The structure of the dorsal body wall of the starfish *Echinaster spinulosus* was studied using polarized light microscopy of frozen tissues, scanning electron microscopy and histology. The collagen fibres of the body wall form a three-dimensional orthogonal web. Voids in the web contain ossicles and papulae. The orthogonal web delivers dimensional stability but allows shear necessary for ray torsion. The ossicles and fibres interact to load the fibres in tension and the ossicles in compression.

Strain rates of the dorsal body wall were measured on live animals during typical movements. Uniaxial tension tests of the body wall yielded Young's moduli of 267 MPa (longitudinal), 249 MPa (transverse) and 353 MPa (bias); curves were essentially linear. The body wall was approximately linearly viscoelastic and showed hysteresis at 0.01 Hz. Stress relaxation over five decades of time (in seconds) yielded relaxation spectra with peaks in relaxation time at 2.96–3.35, depending on test direction. Stress relaxation caused the connective tissue to soften. The surface of fractured stress-relaxed tissue revealed wispy, dissociated fibril tufts, whereas unrelaxed fractures produced blunt-ended fibre bundles. Neural control was necessary for body wall integrity.

Introduction

The body wall of most organisms is often regarded as inert packaging material which serves as a container for the more dynamic organ systems which it contains. However, recent work in the field of biomechanics has revealed that the body wall itself is a significant determinant of an organism's niche, for it determines which movements, methods of feeding and habitats are available to the organism (Armstrong, 1987; Denny *et al.* 1985; Eylers, 1982; Koehl, 1977, 1982, 1984; Koehl and Wainwright, 1977; Vogel, 1981, 1984; Wainwright *et al.* 1976). An investigation of an organism's body wall which determines its structure and mechanical properties can disclose information about factors that determine the geographic and local distribution, energetic limitations and evolutionary constraints faced by that organism. The mechanical properties that yield this information include E or

* Present address: Department of Zoology, University of Western Australia, Nedlands, WA 6009, Australia.

Key words: Asteroidea, collagen, morphology, mechanics.

Young's modulus (stiffness), *in vivo* strain rates (the rate and degree of stretching of the tissue in the organism), ultimate tensile stress (UTS or breaking stress, a measure of the strength of the material), hysteresis (which determines how much energy the material can store) and various time-dependent properties such as the distribution of τ, the relaxation time (which demarcates the elastic *vs* pliant behaviour of the material).

Some of the most interesting and puzzling types of body walls occur among the echinoderms (starfish, sea urchins, sea cucumbers, etc.), whose body walls consist primarily of a collagenous dermis and calcite ossicles. The connective tissue of the echinoderms so far investigated possesses the remarkable property of variable stiffness, which seems to depend on the concentration of ions in the matrix of the collagen (for reviews see Wilkie, 1984; Motokawa, 1984*b*). Eylers (1982) referred to these tissues as mutable collagenous tissue (MCT). Mutable collagenous tissues can change stiffness by over an order of magnitude within several seconds. The change is probably accomplished by neurally mediated variation in the cation concentration of the proteoglycan matrix. Ligaments which consist almost entirely of connective tissue have been most intensively investigated: ophiuroid intervertebral ligament (Wilkie, 1978*a*,*b*), crinoid cirral ligament (Holland and Grimmer, 1981; Wilkie, 1983) holothuroid P-L ligament (Byrne, 1985*a*,*b*,), echinoid spine ligament (Smith *et al.* 1981; Hidaka, 1983) and asteroid spine ligament (Motokawa, 1982*b*). Examinations of the structure and mechanical properties of the entire body wall of echinoderms have been limited to holothurian dermis, which is primarily connective tissue (Byrne, 1985*a*; Eylers, 1982; Greenberg and Eylers, 1984; Motokawa, 1981, 1984*a*,*b*; Motokawa and Hayashi, 1987), and the echinoid test, which is primarily calcareous (Currey, 1975; Harold, 1985; Telford, 1985). The starfish body wall, which contains roughly equal proportions of connective tissue and calcite ossicles, is poorly understood in terms of its structure and mechanics. Eylers (1976) analysed the loading of some of the skeletal elements in the body wall of *Asterias*, emphasizing the stresses that are applied during feeding on bivalves. However, an integrated treatment of all the components of the body wall has not been available. In addition, the evidence for MCT in starfish body wall is fragmentary (Wilkie, 1984).

This paper presents a structural and mechanical analysis of the body wall which forms the dorsal portion of the ray of the starfish *Echinaster spinulosus* (Asteroidea: Spinulosida). *Echinaster* is a common starfish of the Gulf Coast of North America, and occurs on sandy bottoms, eelgrass beds, pilings, rocky rubble and oyster beds. It is an opportunistic predator and scavenger of sponges, ascidians and other sessile macrofauna (Scheibling, 1982). The rays of *Echinaster* feel quite rigid when the animal is handled, and it is difficult to bend or twist the rays by force. However, an undisturbed starfish is able to bend and twist the rays with little apparent effort, which is remarkable considering the paucity of muscle within the ray. The coelomic cavity of the ray is not pressurized, and the animal can still manoeuvre the ray if the body wall has been pierced or cut, as long as major muscles remain intact (P. O'Neill, personal observation), so that changes in

the internal pressure cannot account for the changes in stiffness. Therefore, the explanation for this discrepancy must lie in the mechanical properties of the body wall itself.

Materials and methods

Echinaster spinulosus were obtained from the Gulf Specimen Company (Panacea, Florida, USA). These specimens would be classified as *Echinaster* 'Type 1' by Scheibling's (1982) morphological and size criteria. The starfish were maintained in 250-l aquaria in artificial sea water (Instant Ocean) at room temperature (22–28°C).

A goal of this study was to determine the orientation of the collagen fibres within the dermis in a condition as close to the *in vivo* state as possible. This requirement ruled out most histological procedures, which severely distort connective tissues. All standard fixative mixtures contain ingredients which shrink (ethanol, mercuric chloride, picric acid, formalin) or swell (acetic acid) connective tissue and it is not likely that shrinkage and swelling would be exactly counterbalanced. Shrinkage or swelling represent unacceptable artefacts since they change the dimensions of the tissue and can alter the fibre orientation. In addition, decalcification with acidic mixtures or chelating agents induces connective tissue swelling, and the heat required for paraffin embedding produces severe connective tissue shrinkage (see Putt, 1972). Therefore, the tissues had to be prepared for sectioning without fixation, decalcification or embedding. Instead, pieces of the dorsal body wall were dissected and flash frozen at −40°C with CO_2 to ensure that any ice crystals which formed in the tissue were too tiny to disrupt the connective tissue. The frozen tissue blocks were immediately sectioned in a cryostat at −40°C. Disposable knives were used since the ossicles within the tissue ruined the blades. The sections were placed on slides, thawed, and immediately examined on a Leitz polarizing microscope with rotating stage and first-order red compensator. Measurements of collagen fibres, ossicles, etc. in sectioned material were made on intact material using an ocular graticule on the polarizing microscope. The frozen sections obtained from intact tissue were often obscured by fragments of shattered ossicles. Therefore, for some photographs (Figs 6, 7B, 9), decalcified material was used for clarity of illustration. To determine the volume percentage of the dorsal body wall layers, 10–15 tangential sections of each of the three layers were selected as representative. The relative surface area of each component was determined by projecting the transparency onto paper with a scale mark, tracing the components, cutting them apart, and weighing them. The volume was determined by multiplying the area by the thickness of each component taken from transverse and longitudinal sections.

Muscle and collagen fibres, which are both birefringent, could not be easily distinguished from one another by this method. Therefore, more conventional histological techniques were used to locate and measure the muscles in the dorsal body wall. Procedures were selected which minimized connective tissue distortion

artefacts. Pieces of the dorsal body wall were fixed in 10% formalin buffered with sodium carbonate. Decalcification in 0.5 mol l^{-1} EDTA buffered to pH 7.8 took approximately 3 days for tissue pieces 3 mm thick. After washing in distilled water, the tissue was embedded in gelatin using Pearse's rapid infiltration method at 37°C for 1 h. Gelatin blocks were not hardened with formalin. Sections were cut on a freezing microtome, then floated on warm water to remove the gelatin. After affixing the sections to slides with albumin, they were stained with Elastin–trichrome stain or Weigert's triple elastic tissue stain using phosphomolybdic acid to increase collagen specificity (Gurr, 1962).

For all structural studies, the tissue pieces were centred both longitudinally and transversely on the ray. Studies of ossicles were made in whole animals, strips of intact dorsal body wall and fractured strips of dorsal body wall. The specimens were fixed and dehydrated in absolute ethanol, and the connective tissue was then rendered transparent in methyl salicylate.

Specimens for scanning electron microscopy were fixed in $NaHCO_3$-buffered 10% formalin. They were briefly rinsed in distilled water, air-dried for 1 week at room temperature, coated with 20 nm of Au–Pd, and examined with a Jeol scanning electron microscope.

In vivo strain rates were determined by photographing the starfish as they performed movements in glass aquaria. The time of each shot was measured by recording the camera clicks with a tape recorder. The displacement of the body wall was determined by measuring the distance between marks on the animal's skin. The marks were tattooed onto the animal's skin by a specially constructed tattooing jig which contained cotton threads spaced at 2 mm intervals. The threads were dipped into 1% Methylene Blue and rubbed into the surface of the ray, producing an indelible mark. The marked area was centred on the ray. Animals were photographed on a 1 cm grid which was placed below the glass floor of the aquarium. Some photographs of the animal's underside were taken by photographing the image in a mirror placed under the aquarium.

All animals used for mechanical tests were 7–10 cm in diameter. Handling and measurement of the starfish prior to dissection invariably caused it to stiffen, presumably placing its connective tissue in the 'catch' state. A ray was removed by cutting the base away from the disk. The ambulacral arch was removed by cutting above the adambulacral ossicles. The digestive caeca and gonads were then stripped from the ray interior using forceps. The dissection left an arch-shaped strip of the dorsal body wall which was then trimmed into a strip for mechanical testing. Each test strip contained the point that was centred longitudinally and transversely on the ray. No attempt was made to determine if mechanical properties varied along the ray. The tissue strip was then cut along the appropriate axes for the test (longitudinal, transverse, or bias; see Fig. 1). The ends of each strip were cut larger than the centre portion to facilitate gripping. The width and thickness of the narrow portion of the test specimen were measured to the nearest 0.1 mm with Vernier calipers. The initial length was measured with calipers after the specimens had been mounted in the extensometer, and represented the

distance between the needle-point attachments of the two linearly variable differential transformers (LVDTs, see below).

The tissue strips were dumbbell-shaped to provide large gripping surfaces at the ends. The strips were mounted in an extensometer using padded rubber surfaces on screw-down clamps. One clamp was attached to a fixed carriage and the other to a sliding carriage by braided wire and binding posts. The position of the sliding carriage was altered either by a thumbscrew or by electrical motor. Displacement was measured by two colinear LVDTs attached to the strip by needle points. Force output was delivered by a strain gauge on a cantilever attached to the stationary mount. Force and displacement were recorded on a Brush dual pen recorder. Strain rates for determination of elastic properties were kept in the range 1–2 % s^{-1}, as indicated by the *in vivo* experiments for locomotion.

For stress relaxation experiments, the strips of body wall were bathed in artificial sea water containing 1 % gentamicin sulphate to prevent bacterial degradation during the long-term experiments. When anaesthetized tissues were required, animals were relaxed in 0.1 % MS222 (tricaine methanesulphonate) in artificial sea water for 1 h prior to excision of the test strips. Since echinoderm collagen is known to be sensitive to divalent cations (Wilkie, 1984), which are the basis for many standard echinoderm anaesthetics (e.g. $MgCl_2$), MS222 was substituted. MS222 is a local anaesthetic which depresses the excitability of neurones (Wilkie, 1984), but is unlikely to interact directly with the collagen itself. Tissues that had been anaesthetized were bathed in the same solution during the experiments.

Results are expressed as means±S.E., unless otherwise stated.

Results

Gross anatomy

The body wall forms the surface of the disk and rays of the starfish. It is interrupted on the oral surface by the mouth and ambulacral grooves (Fig. 1A,B). The components of the body wall are an outer epithelium, dermal layer of collagen, calcite ossicles, longitudinal and circular muscles, and an inner epithelium. To facilitate description of the collagen fibres, the body wall was divided into three layers: an ossicle layer sandwiched between an inner and outer dermis (Fig. 1C). The outer dermis (*od*) consisted of the outer epithelium and the layer of connective tissue on the aboral side of the ossicles. It was about 0.22 mm thick. The ossicle layer (*os*) contained the calcareous ossicles and the connective tissue that binds them together, and was about 0.67 mm thick. The inner dermis (*id*) contained the thickest dermal connective tissue layer, the circular and longitudinal muscles and the inner epithelium. It averaged 0.25 mm in thickness. The papulae (dermal gills) which are formed of the two epithelial layers exited between the ossicles through voids in the connective tissue layers. The voids were fairly rigid, with smooth walls (Fig. 2). The largest collagen fibres were visible at low magnification on the surface of the coelomic side of the body wall (Fig. 2).

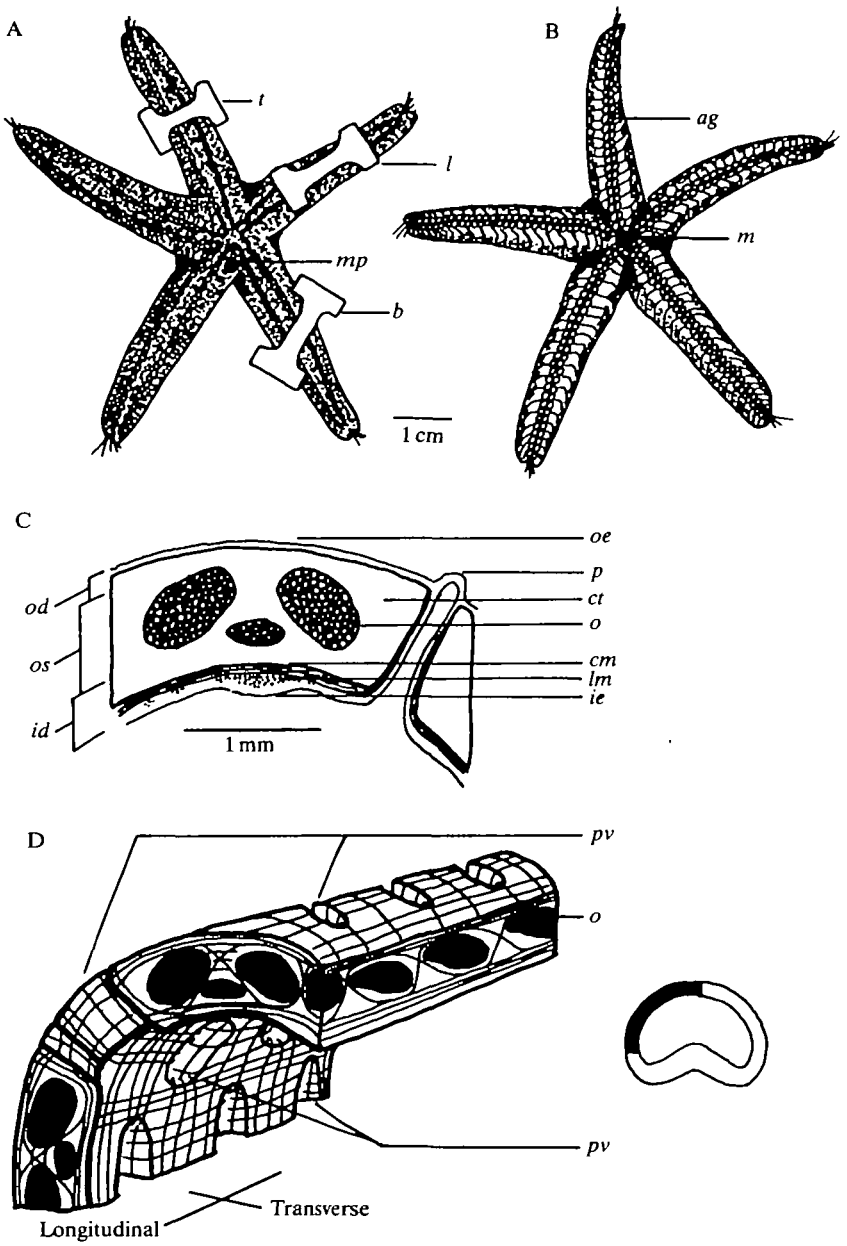

Fig. 1

Musculature

The ray contained two muscle layers attached to the coelomic side of the dorsal body wall. The superficial layer was composed of longitudinal muscles. This layer was poorly defined and varied in depth from 0.01 to 0.06 mm. The thickest part of the longitudinal muscle layer lay directly behind the pigmented apical nerve which marked the inner apex of the ray (see Fig. 2). A sheet of connective tissue

Fig. 1. *Echinaster spinulosus* and the dorsal body wall. (A) Dorsal (aboral) view of *E. spinulosus*. The dark spot on the lower centre of the disk is the madreporite (*mp*). Test strips are shown as they were cut from the dorsal body wall as transverse (*t*), longitudinal (*l*) and bias (*b*) strips. (B) Ventral (oral) view. The mouth (*m*) is in the centre. The body wall is interrupted by the ambulacral grooves (*ag*). (C) Schematic cross-section of the dorsal body wall, divided into the outer dermis (*od*), ossicle layer (*os*) and inner dermis (*id*). The major components of the body wall are: outer epithelium (*oe*), papula (*p*), connective tissue (*ct*), ossicle (*o*), longitudinal muscle thickening (*lm*), circular muscles (*cm*) and inner epithelium (*ie*). (D) Schematic reconstruction of portion of dorsal body wall showing only ossicle (*o*) and connective tissue. Inset shows ray cross-section in which shaded area represents portion shown in diagram. The papular voids (*pv*) are holes which penetrate the body wall to allow respiratory papulae to exit (see also Fig. 2). Collagen fibres (represented by lines) form a three-dimensional orthogonal web.

was often found within the thickened longitudinal muscle strip, and divided the longitudinal muscle into two portions (Fig. 3). When the narrow strip of dorsal body wall containing the longitudinal muscle thickening was excised, *Echinaster* was unable to flex the ray upwards.

The circular muscle layer was always divided from the longitudinal muscle layer by connective tissue which branched to divide the circular muscles into bundles (Fig. 3). The circular muscle layer itself was approximately 0.02 mm thick.

Within the dermis of the ossicle layer were small muscle bundles which connected the reticular ossicles (Fig. 4). They joined ossicles in both longitudinal and circumferential directions; the longitudinal muscles tended to be larger (length approx. 0.027 mm, diameter approx. 0.005 mm) than the circular muscles (length approx. 0.009 mm, diameter approx. 0.002 mm). The muscles did not

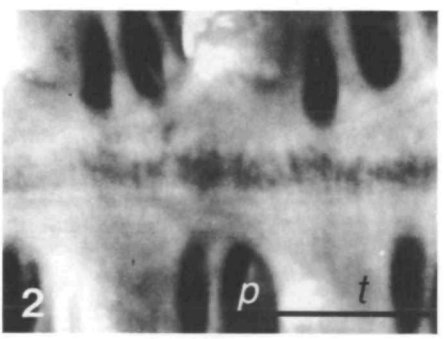

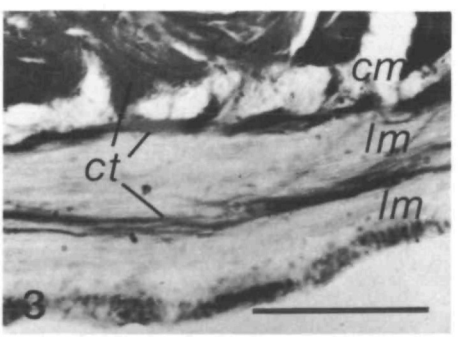

Fig. 2. Low-magnification photomicrograph of the coelomic surface of the dorsal body wall. The central dark strip is the apical nerve which marks the centre longitudinal axis of the ray. The papular voids (*p*) are separated by transverse bars (*t*) of fibrous collagenous connective tissue. The fibres are visible as faint, light striations on the surface. Scale bar, 1 mm.

Fig. 3. Photomicrograph of longitudinal section through the longitudinal muscle thickening beneath the apical nerve. Connective tissue (*ct*) invests the longitudinal muscles (*lm*), as well as separating it from the circular muscles (*cm*) and dividing the circular muscles into strands. Weigert's triple elastic stain. Scale bar, 50 μm.

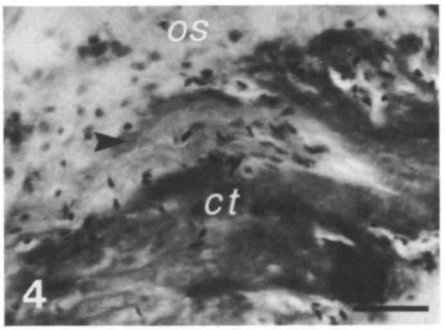

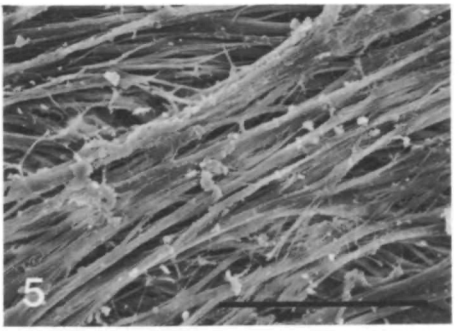

Fig. 4. Photomicrograph of longitudinal section of dorsal body wall showing a reticular muscle (arrowhead). Above the muscle is the stroma remaining from a decalcified ossicle (*os*); below the muscle is a connective tissue (*ct*) strip which intervenes between two ossicles. Weigert's triple elastic stain. Scale bar, 10 μm.
Fig. 5. Scanning electron micrograph of transverse collagen fibres from the inner dermis. The fibres branch and anastomose with adjacent fibres. Scale bar, 100 μm.

insert directly into the calcite, but were connected to the wrapping of collagenous fibres that surrounded each ossicle.

Organization of the collagen

Frozen sections of the intact dorsal body wall, when viewed on a polarizing microscope with a first-order red filter, revealed individual collagen fibres and their orientation. Fibres were traced in serial sections and in photographic records of the sections; over 1200 Kodachrome transparencies of the body wall were studied. Large tracts of collagen were composed of fibres ranging from 0.022 to 0.012 mm in diameter (mean=0.018±0.002 mm, S.E.M.). The fibres appeared to be twisted together, somewhat like rope. Within a fibre, smaller subunits formed a branching, anastomosing network in which the branches were interwoven (Fig. 5). All the fibres were tightly adherent and could not be teased or pulled apart. The fibres were either continuous along the length and breadth of the ray, or were so tightly attached to one another that they appeared to be continuous (Figs 6,7B). Unlike vertebrate collagen fibres, those of *Echinaster* did not have a wavy or crimped appearance when relaxed, although the crimped pattern could be induced by compressing the specimen.

The polarized light studies revealed that the collagen was arranged in a network which was more organized than the 'random feltwork' which was assumed to exist in asteroids (Hyman, 1955). The long axes of most of the fibres were coincident with the longitudinal or transverse (circumferential) axes of the ray, so that an orthogonal web of fibres was formed (Fig. 7A–C). Along the outer edges of each large fibre, smaller branches split off and anastomosed with other fibres (Fig. 5). The transverse and longitudinal fibre tracts of the inner dermis gave off branches which penetrated the thickness of the dorsal body wall, forming radial fibre tracts. Altogether, the collagen of the dorsal body wall resembled a loosely woven, three-

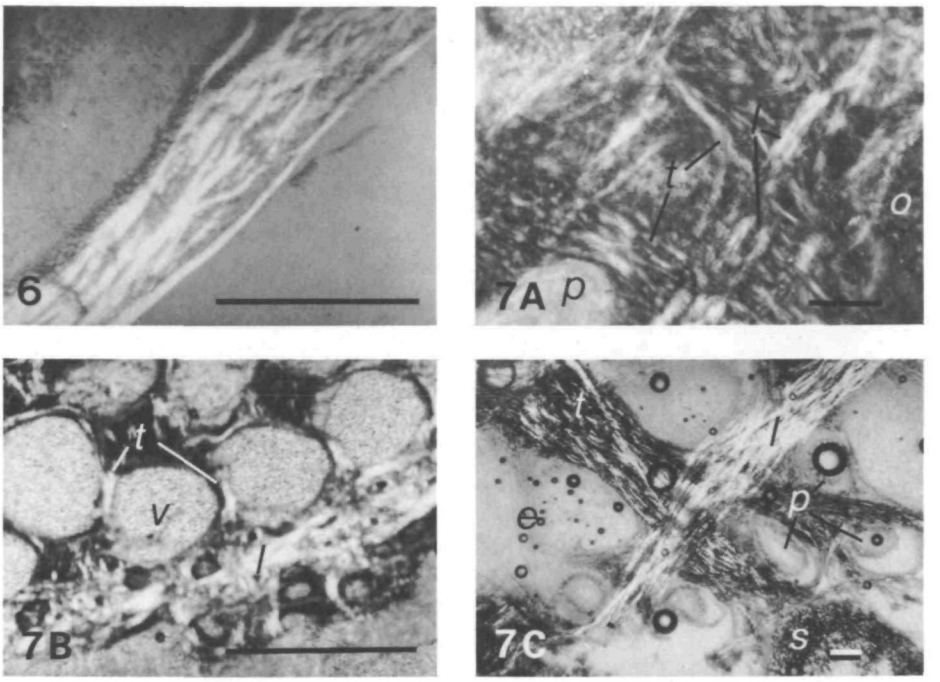

Fig. 6. Polarized light photomicrograph of longitudinal section of dorsal body wall. Tissue was formalin-fixed and decalcified before frozen sectioning. Longitudinal fibres appear to be continuous, although they branch and weave together. Scale bar, 100 μm.
Fig. 7. The orthogonal arrangement of collagen fibres in tangential sections of the dorsal body wall. Photomicrographs were taken in polarized light with a first-order red compensator. (A) The inner dermis, intact frozen section. Scale bar, 100 μm. Thick tracts of longitudinal (*l*) and transverse (*t*) collagen fibres form a dense orthogonal network. The bottom surface of an ossicle (*o*) is visible at lower right. Papular voids (*p*) pierce the entire thickness of the body wall. The labelled void is in approximately the same position as the labelled void in Fig. 2, although this section was taken from deeper within the inner dermis. (B) The ossicle layer. Same photograph as Journal cover. Scale bar, 1 mm. This frozen section was from formalin-fixed decalcified tissue to provide better photographs of the small fibres between the ossicles. A series of voids (*v*) marks the former position of a staggered longitudinal row of ossicles (see Fig. 20F). This row was from the centre longitudinal position of the ray, which would lie beneath the pigmented strip in Fig. 2. This strip of tissue contains no papular voids. The ossicle voids (*v*) are empty but have a grainy appearance due to the ground-glass background. A large tract of longitudinal collagen fibres (*l*) runs alongside the ossicles. Shorter transverse fibres (*t*) run between the ossicles. (C) The outer dermis, intact frozen section. Scale bar, 100 μm. Longitudinal (*l*) and transverse (*t*) fibre tracts are not as dense as in the other layers. The longitudinal fibre tract is at the approximate centre of the ray. Numerous papular voids (*p*) are visible, some of which contain the papulae themselves (ring-shaped structures inside the voids). A sectioned spine (*s*) can be seen at lower right, epidermal tissue (*e*) at centre left.

dimensional fabric in which some of the fibres were 'felted' (frayed together) at their intersections. The intertwining of the fibres ensured that the entire collagen web acted as a single mechanical unit, and that the layers did not delaminate when strained.

The inner dermis was characterized by thick transverse and longitudinal bands of collagen fibres (Fig. 7A). The transverse bands averaged 0.48 mm in width and 0.14 mm in thickness and extended from one papular void to the next (see Fig. 1C). The longitudinal bands were interwoven with the transverse bands; these tracts averaged 0.23 mm in width and 0.20 mm thick. They were continuous along the length of the ray (Figs 6,7B; see also Fig. 20F). The fibres detoured around the voids and could deviate from the main orthogonal axes by as much as 19°. The composition by volume of the inner dermis was 81 % connective tissue, 10 % voids and 9 % muscle and epidermis.

The volume composition of the ossicle layer was 54 % ossicle, 11 % voids, 35 % connective tissue and less than 1 % muscle and other tissue. The collagen fibres of the ossicle layer formed two types of voids: large papular voids which were continuous throughout the body wall thickness (Figs 1D,2), and smaller ossicle voids which were found only in the ossicle layer (Fig. 7B). The ossicles themselves occupied these smaller voids *in vivo*. The large collagen fibres of the ossicle layer generally detoured around or over the ossicles, wrapping them in a three-dimensional orthogonal web. A finer layer of collagen fibres surrounded each ossicle and inserted into the fenestrated structure of the calcite (Fig. 8). These fine fibres formed an outer envelope for each ossicle so that there was no calcite/calcite contact between ossicles. This envelope appeared to be loosely attached to the larger fibres forming the orthogonal network, since in dissections of fresh material it could easily be torn from them. In addition, these fibres accepted counterstaining with facility in the Masson Trichrome technique, which indicated that this

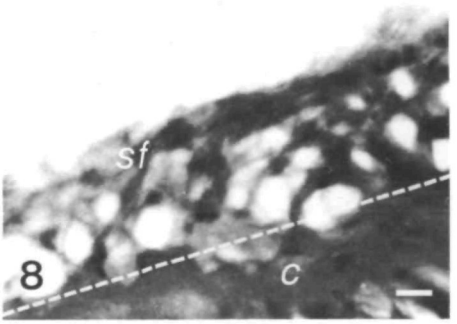

Fig. 8. Photomicrograph of collagen–ossicle junction. Small collagen fibres (*sf*) invade the spaces of the fenestrated calcite of the ossicles. In the decalcified material, the junction has a lacy appearance. Ossicle border, before decalcification, is marked by the dashed line. The stereom is no longer present. Large fibre tracts are indicated by *c*. Elastin trichrome stain. Scale bar, 10 μm.

connective tissue was less dense than the surrounding larger fibres (Lanir *et al.* 1984).

The largest longitudinal fibres of the ossicle layer appeared to be continuous along the length of the ray (Fig. 7B). The transverse fibres appeared to run only from one ossicle to the next in tangential section, but transverse sections revealed that these fibres went either over or under the ossicles and then continued in the transverse direction.

The fibre array of the outer dermis was relatively flimsy compared with that of the other layers. The fibre tracts were more widely spaced and made large deviations from the orthogonal axes as they wrapped around the bases of the spines that protrude from the starfish's surface (Fig. 7C). The volume composition was 63 % collagen fibres, 2 % ossicles, 15 % voids and 20 % epidermis, gelatinous matrix or mucus glands.

Radial fibres tied all three layers of the dorsal body wall together. Most of the radial fibres originated as transverse fibres or short longitudinal fibres of the inner dermis (Fig. 9, see also Fig. 1D). Some fibres ascended the walls of the papular voids and reached the outer dermis, where they generally continued in the direction that they had pursued in the inner dermis. Other radial fibres penetrated solid masses of collagen; their fate in the outer dermis was difficult to determine.

The total volume composition for the entire dorsal body wall was 51 % connective tissue, 32 % ossicles, 11 % voids and 6 % epidermis, muscle, mucus glands and other mechanically insignificant components.

Organization of the ossicles

The dorsal body wall of spinulosid asteroids contains the dorsolateral and carinal ossicles (Hyman, 1955); however, in *E. spinulosus* these were indistinguishable. Instead, there were two different ossicle shapes: oblate disks and ellipsoid bars. These ossicles form a reticular lattice consisting of more-or-less hexagonal rings (see Fig. 20H). Generally, the rings were composed of six oblate disks and two ellipsoid bars, but variations of 5–7 disks and 2–4 bars were

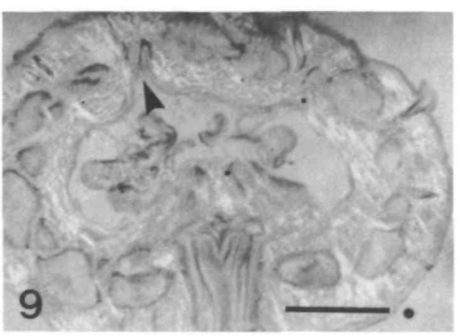

Fig. 9. Polarized light photomicrograph of cross-section of ray. Transverse fibres (in white) can be observed ascending the walls of a papular void (arrowhead) as they become radial fibres. Unstained decalcified section. Scale bar, 1 mm.

common. Some individuals, particularly larger specimens, seemed to have more orderly skeletons than others. The hexagonal rings surrounded the voids where the papulae exited. The rings interlocked in a staggered fashion, forming alternating longitudinal rows of papulae and double ossicles (see Fig. 20F).

In vivo *strain rates*

Prior to mechanical testing, the *in vivo* strain rates for the dorsal body wall were determined, so that the mechanical tests could be performed within the biologically relevant range. When *Echinaster* was at rest on a horizontal surface, the primary stresses on the dorsal body wall were transverse tensile stresses generated by the animal's own weight (Fig. 10A). In the vertical resting position, as occurs when the starfish is clinging to a rock or the wall of the aquarium, the principal stresses in the dorsal body wall were longitudinal tensile stresses in arms *A*, *C* and *D*, and transverse tensile stresses in arms *B* and *E* (Fig. 10B). In unanaesthetized animals, there was no discernible stretching of the dorsal body wall in either situation. *Echinaster* can remain motionless for many hours, or even days, without appreciable strain in the dorsal body wall.

Normal locomotion consisted of creeping along a horizontal substratum using the tube feet. The dorsal body wall remained rigid during this movement, but was subjected to transverse stresses from its own weight (Fig. 10C). In addition, the action of the tube feet could generate small tensile or compressive stresses. Strain rates were measured for horizontal crawling on a smooth glass surface. Longitudinal tensile strain rates averaged $0.013 \pm 0.002\,s^{-1}$ ($N=54$) and longitudinal compressive strain rates averaged $0.017 \pm 0.003\,s^{-1}$ ($N=27$).

Echinaster explores its environment and feeds by bending and flexing its rays. The nomenclature used to describe ray movements are the standard terms employed by kinesiologists to relate movements of an appendage relative to the

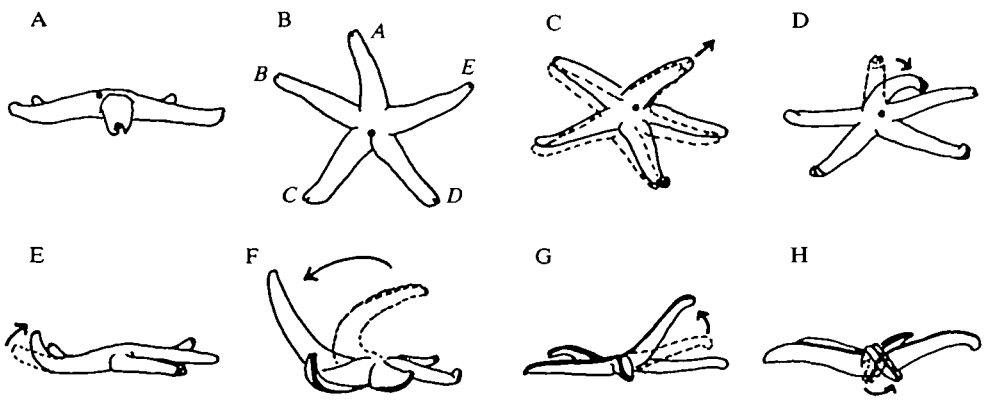

Fig. 10. Movements of *Echinaster spinulosus* which load the dorsal body wall. The dark spot is the madreporite. (A) Horizontal resting. (B) Vertical resting (rays are designated by Carpenter's system). (C) Walking on horizontal surface. (D) Lateral bending of ray. (E) Ray flexion. (F) Ray extension. (G) Ray hyperextension when animal is lying on its dorsal surface. (H) Ray torsion during righting. See Table 1.

body (Wells, 1966). In ray flexion (Fig. 10E), the dorsal body wall experienced compressive longitudinal stress, while the ventral surface was stretched. In extension (Fig. 10F), the dorsal wall was released from compression and returned to its neutral position. In ray hyperextension (Fig. 10G), the dorsal body wall was stretched longitudinally, generating tensile stress, while the ventral surface was compressed. In lateral bending (Fig. 10D), half the dorsal body wall was loaded in longitudinal tension and the other half was loaded in compression. The strain rates for these movements are summarized in Table 1.

Flexion takes the longest time of any of these ray movements, but it is probably limited by the stiffness of the ventral (oral), not the dorsal, body wall. The ventral body wall dissected from fresh, handled animals is quite stiff in tension but is easily compressed (P. O'Neill, unpublished observation); it contains large ambulacral and adambulacral ossicles linked in series by muscle and connective tissue. Compression of the dorsal body wall is relatively easy for the animal – the body wall simply buckles in several areas. Likewise, extension is rapid since the dorsal body wall is not really being stretched but is merely being pulled taut again as the ray falls back into the resting position and the ventral body wall is released from tension. Hyperextension, however, directly stretches the dorsal body wall by up to 13%; the ventral body wall is compressed. It appears to be a difficult exercise for the animal, which will avoid climbing over obstacles or depressions where hyperextension is required. Hyperextension most commonly occurs during righting, with the animal resting on its dorsal surface as a ray is raised in an attempt to locate a substratum. Hyperextension could only be induced in other circumstances by supporting the animal's disk on a pedestal and leaving the rays unsupported, affording no other means of escape.

The most complex ray movement occurs during righting. *Echinaster* generally rights itself by the rotation of one ray by 180° (Fig. 10H), which places the ray in torsion and induces complex shear stresses in the body wall. Once the ray is rotated, the tube feet attach to the substratum, and the rest of the body is slowly rotated by the attached arm and pulled over until the ventral surface contacts the substratum. This process generates large torsional moments on the ray and the dorsal body wall, and is probably the most severe type of load that the body wall must bear. It took the ray about 4.5 min to complete its full rotation, yielding a torsion rate of $0.70\pm0.1°\,s^{-1}$ ($N=10$). It generally took 3–7 min for the body to rotate to complete righting. Torsion loads the dorsal body wall in shear, which can be resolved into a longitudinal tensile stress and a transverse compressive stress. During torsion, the strain rate of the longitudinal component averaged $0.009\pm0.002\,s^{-1}$ ($N=10$) and the transverse component averaged $0.001\pm0.0002\,s^{-1}$ ($N=10$).

Mechanical properties

Micro-stretch experiments were performed by stretching 40 μm thick sections of the dorsal body wall while observing the sections with a polarizing microscope. As the sections were stretched, at first the papular voids collapsed, then the collagen

Table 1. In vivo *movements and strain rates*

Rate of movement	Time for maximum displacement	Loading of dorsal body wall	Strain rate of dorsal body w (s^{-1})
$1\,cm\,s^{-1}$	–	Tension and compression	0.013 ± 0.002 (tensio 0.017 ± 0.003 (comp
$0.6\pm0.09°\,s^{-1}$	150 s for 90°	Compression	-0.004 ± 0.001
$5.3°\,s^{-1}$	17 s for −90°	'Tension'*	0.007 ± 0.003
$3.3\pm0.8°\,s^{-1}$	27 s for 90°	Tension	0.005 ± 0.001
$3.8\pm0.8°\,s^{-1}$	24 s for 90°	Tension on abducting surface Compression on adducting surface	0.024 ± 0.005 (tensio 0.038 ± 0.010 (comp
$0.70\pm0.1°\,s^{-1}$	257 s for 180°	Shear (resolved into longitudinal tension and transverse compression)	0.009 ± 0.002 (longitudinal com 0.001 ± 0.0012 (transverse comp

S.E.

ckles are being released, no actual tensile loads develop.

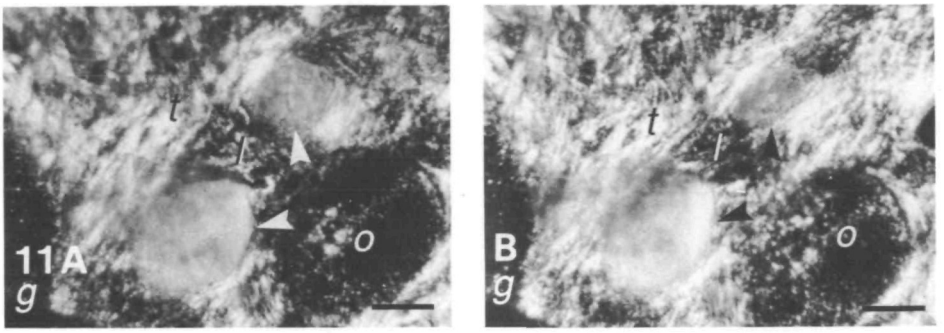

Fig. 11. Polarized light photomicrographs of a micro-stretch experiment. Tangential section of ossicle layer from intact frozen tissue. *g*, microgrip; *o*, ossicles. The papular voids are indicated by arrowheads. The transverse axis runs from the upper right corner to the lower left corner. *t*, transverse fibres; *l*, longitudinal fibres. (A) Unstretched section. (B) Section stretched in the transverse direction. Papular voids become narrower. Collagen fibres distort in the direction of pull, as indicated by a shift to a lighter shade in the photograph. In polarized first-order red light, the colour changes from orange to yellow.

fibres stretched slightly (Fig. 11A,B). There were no significant differences in the behaviour of sections in the longitudinal or transverse directions, but the collapse of the papular voids was more pronounced when the sections were stretched on the bias. The fibre tracts did not slide past one another, indicating that the junctions between longitudinal and transverse fibres were tightly bound.

Hookean properties

The elastic mechanical properties of the dorsal body wall were investigated by performing uniaxial tension tests on an extensometer. Strips of the body wall were tested in the longitudinal, transverse and bias directions (Fig. 1A). Strain rates were kept in the range 1–2 % s^{-1}, which corresponded with the range for normal locomotion.

The stress–extension curves for all three test directions are essentially linear (Fig. 12), with the exception of a J-shaped base in the curve for the bias direction. Past the toe of the bias curve, there is no significant departure from linearity, as for the other two curves ($P>0.95$). Young's modulus was calculated as the average slope of the linear portions of the curves. The data on Young's modulus, ultimate tensile stress and ultimate tensile strain are summarized in Table 2. The overall linearity of the curves indicates that the dorsal body wall behaves in an essentially Hookean fashion at this strain rate. The difference in E between the longitudinal and transverse directions is not large, but it is statistically significant ($P<0.05$, Tukey's ANCOVA). The bias direction E is significantly greater than either of the other two directions ($P<0.05$).

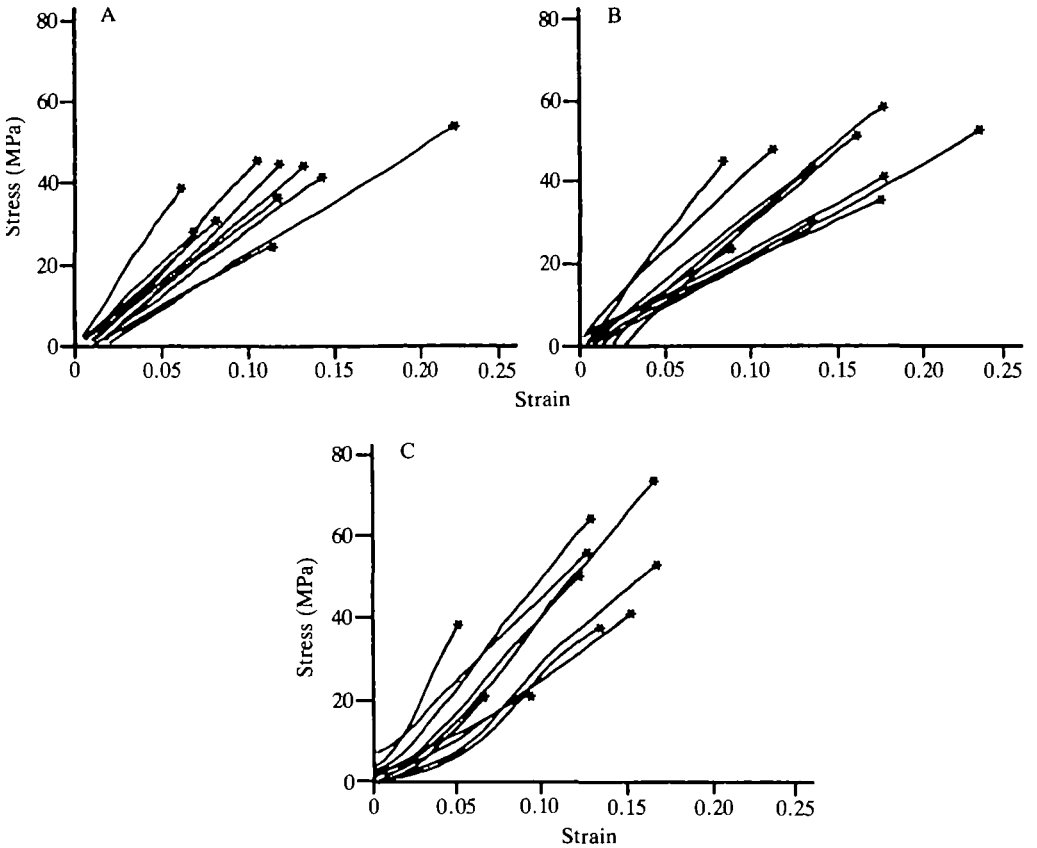

Fig. 12. Stress–strain data for the dorsal body wall loaded in tension at strain rates of 1–2 % s^{-1}. Asterisks indicate specimen failure. (A) longitudinal loading; (B) transverse loading; (C) bias loading.

Table 2. *Elastic properties of* Echinaster *dorsal body wall*

	Test direction		
Parameter	Longitudinal	Transverse	Bias
Young's modulus (MPa)	266.7±13·3* (N=10)	248.7±17.7* (N=10)	353.3±20.0* (N=10)
Ultimate tensile stress (MPa)	37.1±2.8 (N=10)	43.5±3.7 (N=10)	45.1±5.8 (N=10)
Ultimate tensile strain (%)	11.7±1.5 (N=10)	14.6±1.5 (N=10)	11.6±1.3 (N=10)

* Significantly different $P<0.01$ (Tukey's Q).
All parameters measured at $d\epsilon/dt=0.01-0.02\,s^{-1}$.

Fig. 13. Fracture surface resulting from rapid tensile failure of a fast-fractured collagen bundle, loaded in the bias direction. Polarized light micrograph of tangential frozen intact specimen. This bundle was part of a transverse bar analogous to that indicated by *t* in Fig. 2. The transverse direction runs from lower left to upper right. The bundle fractured in the typical layered fashion; arrowheads indicate broken ends of four layers, two transverse and two longitudinal. Collagen fibres have blunt tips. Scale bar, 100 μm.

Fast fracture

Failure of the specimens occurred by sudden fracture of the dermal collagen, with no necking or plastic flow. The large fibre tracts were torn across their narrow portions. Various sublayers of the fibre tracts usually tore in a layered, stair-step fashion. The individual fibres were torn in blunt-ended bundles (Fig. 13). Ossicle fracture was common only in bias loading. Ossicles were usually not pulled from their original positions, but were generally cracked at their mid-sections, with the surface envelope of fibres attached to the ossicle but stripped away from the larger fibres, indicative of failure in compression (see Discussion). The breaking stresses for the three different directions were not significantly different ($P>0.95$, ANCOVA), although the longitudinal breaking stress was slightly less than that in the other two directions (Table 2).

Viscoelastic properties

Virtually all biological materials exhibit some time-dependent properties, which means that the E may vary by as much as several orders of magnitude depending on the strain rate and previous history of the material. Generally, when loads are applied slowly, biological materials tend to be soft and pliant, like viscous liquids. When loads are applied quickly, they act as stiff and elastic solids. In other words, they have *viscoelastic* properties (Dorrington, 1980; Wainwright *et al.* 1976).

Hysteresis

A Hookean material is one which is perfectly elastic, that is, all the energy which is put into it when it is strained is released when the material returns to its original dimensions. Thus, the loading and unloading curves can be perfectly superimposed, and the material is perfectly resilient. Some materials, however, lose

some of the strain energy (as molecular rearrangements, heat, etc.) when they are stretched; such materials show a mechanical hysteresis. The difference between the loading and unloading curves indicates the amount of energy lost. A material with a large hysteresis tends to remain deformed, since there is insufficient strain energy to return it to its original state.

The dorsal body wall of *Echinaster* was tested in all three directions for hysteresis at frequencies of 10, 1, 0.10 and 0.01 Hz. Each loading and unloading constituted one cycle. The body wall showed essentially Hookean behaviour at the three higher frequencies, but produced a hysteresis at 0.01 Hz. At this frequency, the low strain rate (around 0.0004 s^{-1}) allowed the material to enter a viscous state and lose much of the strain energy. In the longitudinal direction, the body wall lost 50±3 % (N=3) of the stored energy. When tested in the transverse direction, 44±3 % (N=3) of the energy was lost; in the bias direction, 28±3 % (N=3) was lost. Greater resilience on the bias direction is expected, since the load is distributed to both sets of fibres. Fig. 14 shows the hysteresis loops for one of the three individuals tested.

Linear viscoelasticity

Viscoelastic behaviour may be linear or nonlinear. Application of simple linear viscoelastic theory, such as data analysis employing Maxwell or Voigt (spring and dashpot) models, is appropriate only if a material obeys the Boltzman superposition principles (Wainwright *et al.* 1976; Dorrington, 1980). For example, a linearly viscoelastic material has a time-dependent modulus, $E_t=\sigma_t/\epsilon$ (where σ_t is stress at time t over a constant strain), which should be constant when measured at a particular value of t, regardless of the initial load placed on the specimen. Linear

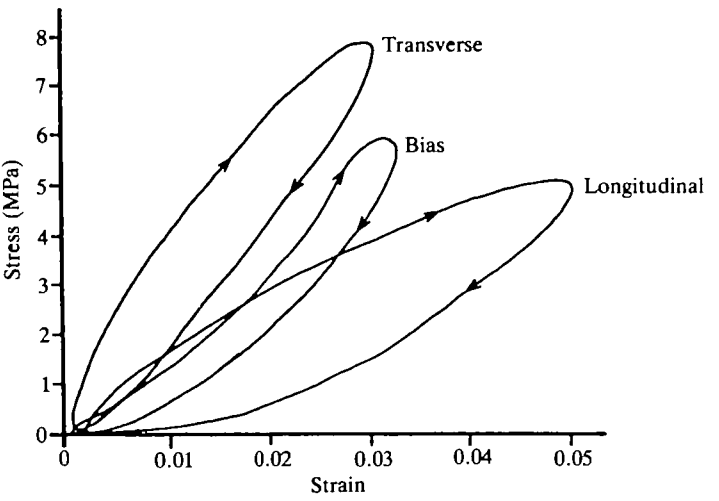

Fig. 14. Hysteresis for the dorsal body wall at 0.01 Hz. The graph shows typical results from three strips of tissue taken from one individual. The loading curves are marked by upward arrows; unloading curves by downward arrows.

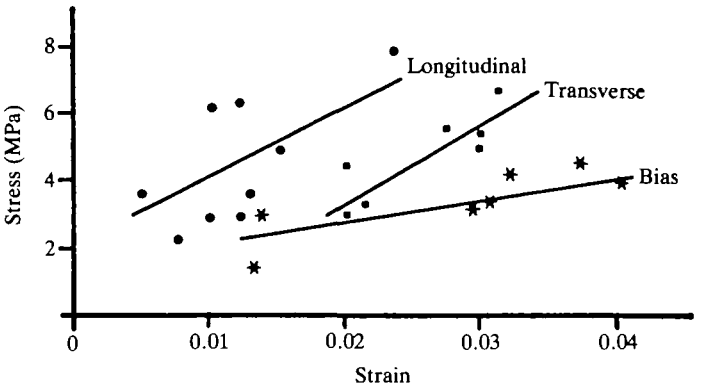

Fig. 15. Isochronal plots of stress relaxation data taken for $t=100$ s. Longitudinal loading, circles; transverse loading, squares; bias loading, asterisks. Lines represent the least-squares linear regression through each set of points; all regressions are significant (F-test, $P<0.05$).

viscoelastic behaviour can be checked by making isochronal plots taken during stress relaxation experiments (Dorrington, 1980). An isochronal plot shows σ_t *vs* ϵ_t at a certain fixed time during stress relaxation from specimens that were loaded with different initial stresses. If the material is linearly elastic, the isochronal plot will be a straight line. Isochronals taken at other fixed times should also be linear. Isochronals for the dorsal body wall in each test direction were plotted for $t=1$, 10, 100 and 1000 s for stress relaxation data from anaesthetized tissue (see below). An example for $t=100$ s is shown in Fig. 15. A significant linear correlation was obtained for each test direction ($P<0.05$), although the scatter in the points was marked due to the variability between specimens. For the purposes of the present study, linear viscoelastic theory was assumed to be an acceptable approximation until further work can demonstrate a clear alternative.

Stress relaxation

Stress relaxation refers to the decay of stress with time while a specimen is held at constant extension. When a viscoelastic material is held at a constant extension, the mechanical energy is dissipated as fibre sliding, straightening of molecular side chains, bond stretching or breaking, heat, etc. When the material is released, it does not return to its original dimensions immediately. If all bonds are intact, it may eventually restore itself; if not, the material will exhibit some permanent, or plastic, deformation. Stress relaxation experiments offer a way of distinguishing between the elastic and viscous properties of the material.

The stress relaxation curve usually plots the modulus that the material is exhibiting at the time (E_t, the time-dependent modulus) *vs* log time (Fig. 16A). Sections of the stress relaxation curve which show a rapid change in slope characterize the times at which the major molecular transformations occur in a

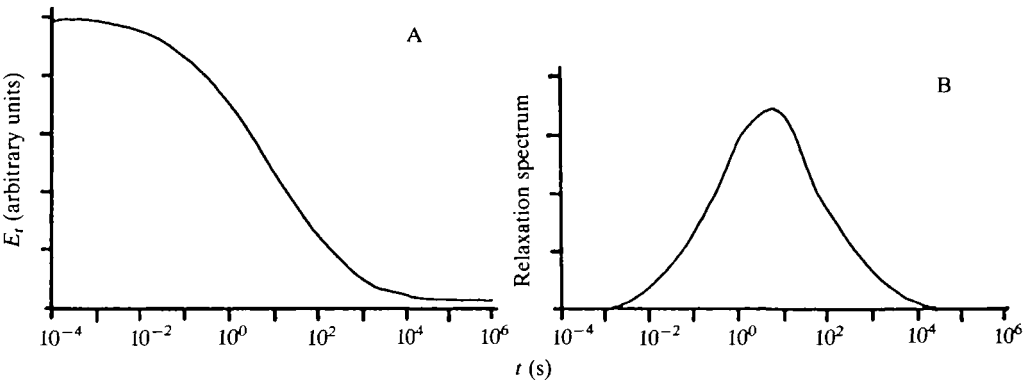

Fig. 16. Idealized stress relaxation curve (A) and relaxation spectrum (B) (after Alfrey and Doty, 1945). A linearly viscoelastic material is subjected to an instantaneous deformation which is held constant at $t=0$. The decay of the resulting stress is plotted against log$t$. For the imaginary material shown here, behaviour is essentially elastic (Hookean) between 10^{-4} and 10^{-1} s; the material is glassy. The major change (glass transition) occurs between 10^{-1} and 10^{3} s. During this interval, most of the strain energy is released and the material becomes pliant. From 10^{3} s onwards, the material behaves as a viscous liquid. The relaxation spectrum illustrates the proportion of the relaxation events occurring at a particular time, τ, measured on the same log$t$ scale. Complex materials are always expected to yield broad spectra.

material. The distribution of these events is delineated by the relaxation time, τ, for the material. A material in which a single event accounts for relaxation will have but a single relaxation time which will separate the elastic and viscous realms of behaviour. At times less than τ, the material is essentially elastic. At times greater than τ, the material flows like a viscous liquid. At times which coincide with τ, the material can exhibit rubbery, leathery or plastic behaviour. Many materials are characterized by several events during stress relaxation. These types of materials will have a number of relaxation times, one for each relaxation event. Their stress relaxation curves will resemble a staircase, with a 'step' associated with each event. Biological 'materials', which are generally complex composites, are expected to have even more complicated relaxations. The stress relaxation curve may show a gradual change in slope (e.g. Fig. 16A). There may be so many relaxation events, each with its own τ, that delineation of separate times is impossible, and the τ values merge into a continuous distribution, the relaxation spectrum (Fig. 16B). Determination of relaxation times for materials like this by conventional spring and dashpot models is neither practical nor accurate (Dorrington, 1980). However, the Alfrey approximation (Alfrey and Doty, 1945), which assumes the material has an infinite number of relaxation times, can be used. The relaxation function, κ' (logτ), is the proportion of the total change in slope of the stress relaxation curve which occurs at time τ. The curve determined in this w[illegible] (Fig. 16B) is the relaxation spectrum, and its peak (τ_{max}) coincides with the

greatest change in the relaxation behaviour and represents the time around which most of the relaxation events cluster. When $t \ll \tau_{max}$, the material is elastic, and when $\tau \gg \tau_{max}$, the material is viscous. The realm of leathery or pliant behaviour is broader than in simple viscoelastic materials and is a function of the variance of the relaxation spectrum.

Stress relaxation experiments were performed in the three principal test directions (Fig. 17). Imposed extensions were in the range 5–8 % to ensure that the tissue was not damaged in any way. Initially, the tests were performed on fresh, unanaesthetized tissue (Fig. 17A). However, it became apparent that the tissue required anaesthesia during these long-term (>24 h) experiments, since the smooth muscle present in the body wall contracted and severely deformed the specimens. The specimens always curled in the transverse direction, never longitudinally, which indicated that the deformations were caused by the circular muscles. Scraping as much muscle as possible off the coelomic side of the test strips did not eliminate the contractions. The contractions introduced severe stress concentrations within the body wall so that the specimen was no longer being stressed in the desired direction. Experiments on unanaesthetized tissue in the transverse and bias directions were unsuccessful. The muscle contractions caused an increase in the force readings and pulled the grips out of alignment, rendering the data useless. Therefore, all further stress relaxation experiments were performed on tissues anaesthetized with MS222.

The stress relaxation curves presented in Fig. 17 are averages taken from 7–10 tests made in each direction on anaesthetized tissue, and three tests on unanaesthetized tissue. Complete relaxation took approximately 10^5 s for the dorsal body wall. For all stress relaxation results t is given in seconds. The effect of anaesthesia was primarily quantitative; Fig. 17A (unanaesthetized) and Fig. 17B (anaesthetized) have similar shapes. The major difference between them was the greater proportion of early relaxation events (between $\log t \approx 0.4$ and 1.8) for unanaesthetized tissue. The results for anaesthetized tissue in the three directions were all similar. For the first 10 s or so, the dorsal body wall behaved as a simple elastic solid, and even for the first 5 min ($\log t \approx 2.5$), behaviour was still largely elastic. Then, when 15–17 min had elapsed ($\log t \approx 3.0$), the modulus had dropped by 50 %. The stress decayed to low levels between 1.5 and 3 h ($\log t \approx 3.8$–4.0), when the dorsal body wall assumed a soft, plastic phase. A visible transition accompanied the plastic phase. The dorsal body wall was normally a shiny, translucent whitish colour; after stress relaxation, it changed to a dull, opaque white.

The relaxation spectra (Fig. 17) were determined by the Alfrey approximation (Alfrey and Doty, 1945). The use of the approximation was justified since the stress decayed over more than 1.5 decades of time and showed no sharp discontinuities (Dorrington, 1980). The peaks in the relaxation spectra fell at $\log \tau = 3.22$ for unanaesthetized, longitudinal tests, and at $\log \tau = 2.96$, 3.35 and 3.32 for anaesthetized tests in the longitudinal, transverse and bias directions, respectively. The relaxation spectra were all similarly asymmetrical, being skewed to the left.

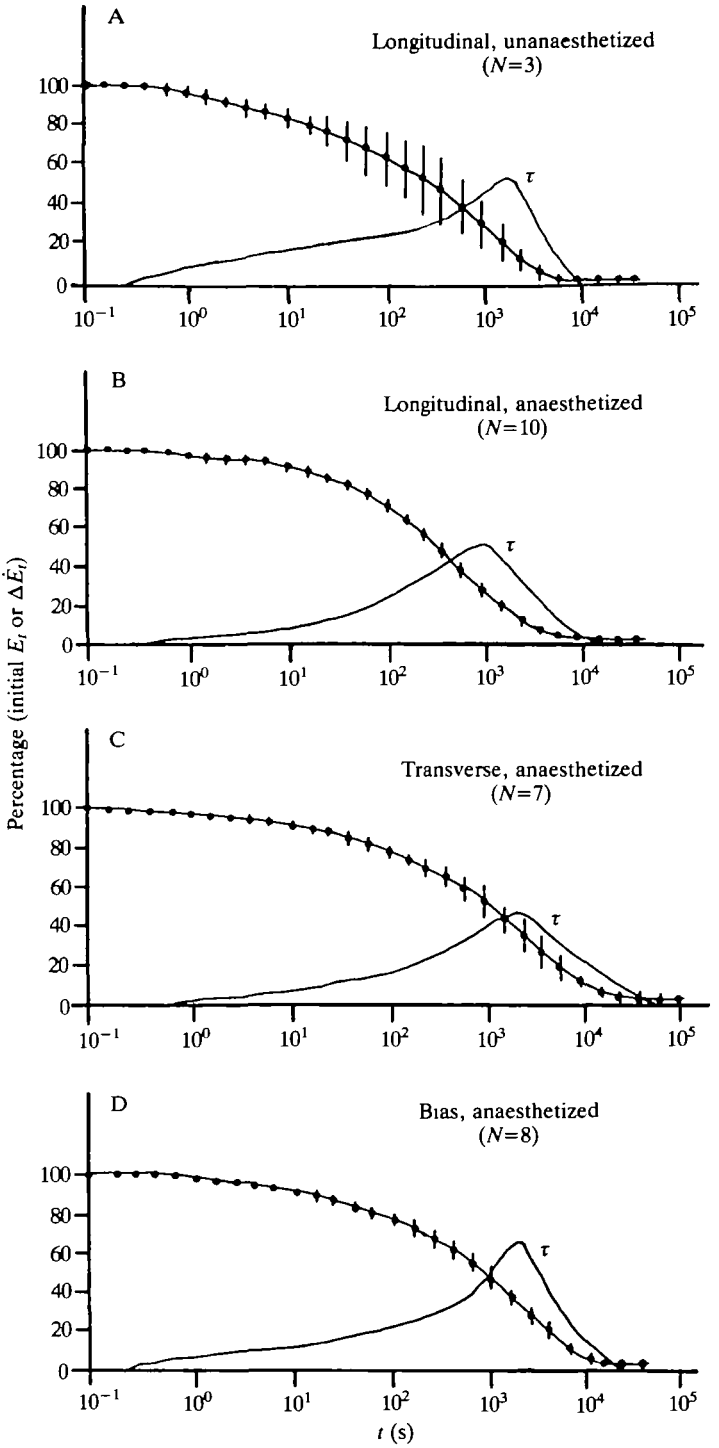
A
Longitudinal, unanaesthetized
(N=3)
B
Longitudinal, anaesthetized
(N=10)
C
Transverse, anaesthetized
(N=7)
D
Bias, anaesthetized
(N=8)
τ
Percentage (initial E_I or ΔE_I)
t (s)

Fig. 17

Fig. 17. Stress relaxation curves (upper line in each graph) and relaxation spectra (lower line in each graph) for the dorsal body wall. All points are ±1 S.E.

Relaxed fractures

The stress decayed to low levels by $\log\tau=4.0$, and reached an equilibrium, E_R, the relaxed modulus. The values of E_R were low, around 1 MPa, and close to the limits of resolution of the equipment. To ensure that the tissue had not lost mechanical integrity, some of the stress-relaxed specimens were subjected to tensile fracture (without being removed from the extensometer). These specimens were strained at 1 % s^{-1} until fracture, following the protocol of the tension tests. The average breaking stress of relaxed specimens was 5±0.9 MPa ($N=15$), with no significant differences between the test directions.

The fractured specimens were frozen, sectioned, and examined on the polarizing microscope. These fracture surfaces were clearly different from those produced in unrelaxed tissue (Fig. 18A). The collagen fibre bundles were pulled apart into tiny fibres, about 4–10 μm in diameter. The fibres gave the relaxed fracture surfaces a wispy, shredded appearance (Fig. 18A,B). Further back from the fracture surface, the collagen fibres showed clear evidence of plastic flow through the matrix (Fig. 18C).

Anaesthesia in whole animals

The stress relaxation experiments indicated that the starfish's body wall would ultimately assume a nearly fluid state under prolonged loading. Since the animals were capable of remaining motionless for long periods without apparent strain in the body wall, it was clear that, in the intact animal, some process must act to prevent stress relaxation of the connective tissues when the animal is motionless. These observations led to the hypothesis that active neural modulation of the body wall was necessary to prevent disintegration. The hypothesis was tested by suspending healthy animals in an aquarium from a padded clamp on one ray. The control animals were immersed in artificial sea water, while the experimental animals were immersed in artificial sea water containing 0.1 % MS222. The results (Fig. 19) verify the role of neural control in maintaining body wall integrity. Anaesthetized animals 'melted.' In both control and anaesthetized animals, the clamped ray bore the full weight of the body since the animals were unable to reach the sides of the aquarium. In both groups, creep occurred in this ray. Although measurements were taken only of the dorsal body wall, the ventral body wall was obviously stretching at the same rate. The onset of discernible stretching occurred at approximately the same time (about 30 min) in both groups, although the degree of deformation was far greater in anaesthetized animals.

In control animals, the free rays writhed throughout the experiment, presumably in an effort to locate a substratum. These arms did not lengthen appreciably, but only experienced local tension and compression associated with the writhing movements. The clamped arms of these animals steadily elongated throughout the

experiment, averaging a strain rate of 0.10±0.01 % min^{-1} (N=3), and reached an average strain of 44.4±6.7 % (N=3) immediately prior to fracture at 7.5 h. The clamped arms always broke cleanly at the site of the clamp. The animals then crawled away, and returned to normal behaviour.

In anaesthetized animals, all arms elongated (Fig. 19). The animals became quiescent about 30 min after being placed into the aquaria, and the clamped arm began to stretch. The free rays lost rigidity and began to droop after about 1 h. Stretching continued at a fairly steady rate, averaging 0.17±0.02 % min^{-1} (N=3) for clamped arms and 0.05±0.02 % min^{-1} (N=12) for free arms. The maximum elongation of the clamped arm reached 76.03±3.5 % (N=3) and for free arms reached 21.81±0.08 % (N=12). Fracture occurred after 7.5–8 h, when the

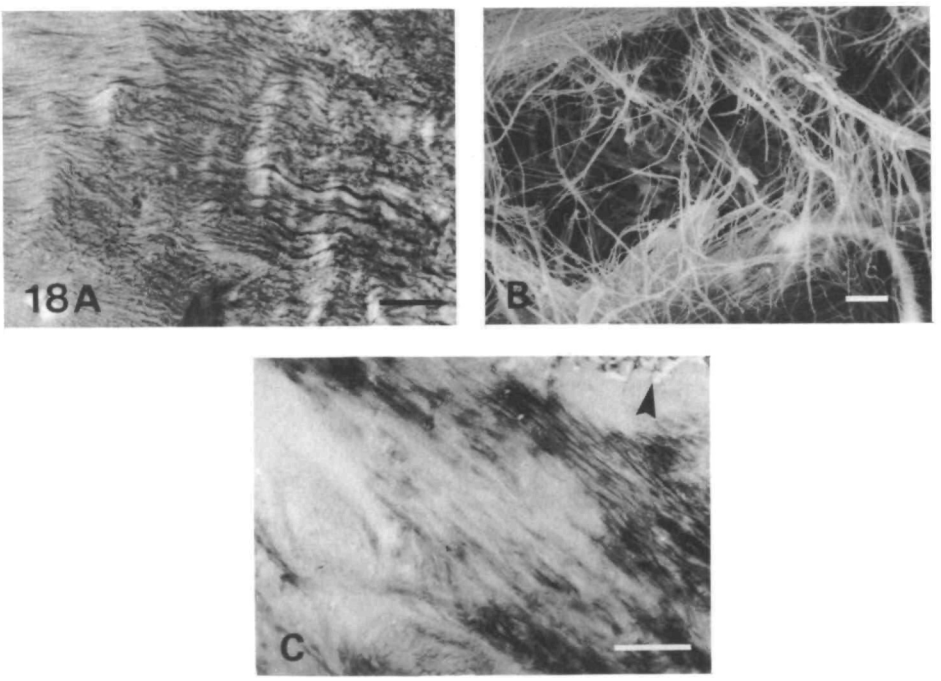

Fig. 18. Fracture surfaces of connective tissue subjected to stress relaxation prior to tensile fracture. (A) Polarized light micrograph of a tangential frozen intact section of transverse collagen bundle from the inner dermis. The tissue was stress-relaxed and fractured in the transverse direction (approx. left to right). The collagen fibres were wavy and dissociated (compare Fig. 13). The fracture surface shows wispy, frayed fibrils (left edge). Scale bar, 25 μm. (B) Scanning electron micrograph of the wispy frayed fibrils similar to those in A. The smaller fibrils appear to have unravelled or peeled away from the larger fibre bundles. Scale bar, 10 μm. (C) Polarized light micrograph of tangential frozen intact section of a transverse fibre bundle from the inner dermis. The tissue was stress-relaxed and fractured in the transverse direction (the transverse axis runs from upper left to lower right). The two large light areas on the left are papular voids. Fibres have dissociated and been pulled away from the ossicle (arrowhead) and have been sheared through the matrix, indicating plastic flow. Scale bar, 100 μm.

clamped arm shredded in a ragged fashion around the clamp site. The anaesthetized animals remained motionless on the floor of the tank. They recovered normal mobility within 1 h of being placed back into artificial sea water, and their body dimensions returned to normal after 24–36 h.

Intact animals resting horizontally and subjected to anaesthesia were also observed to collapse under their own weight even though they were completely immersed in water. When the starfish was in a horizontal resting position, the dorsal body wall was stressed in the transverse direction and the ray flattened. This deformation was also fully reversible, and the animals recovered their original dimensions within 24 h of being placed back into fresh artificial sea water.

Discussion

Most cylindrical biological structures are expected to contain layers of circular and longitudinal muscles (Wainwright, 1982, 1988). The dorsal body wall of *Echinaster spinulosus* departs from this pattern. The dorsal body wall musculature can be divided into two functional parts: the reticular muscles, which were embedded within the connective tissue, and the superficial musculature, which was found outside the main connective tissue layers. The function of the reticular muscles in *Echinaster* remains obscure. It has been suggested that reticular muscles lock the skeleton into a rigid framework in the starfish *Asterias* (Eylers, 1976; Christensen, 1957; Kerkut, 1955). A strong, rigid framework depends upon

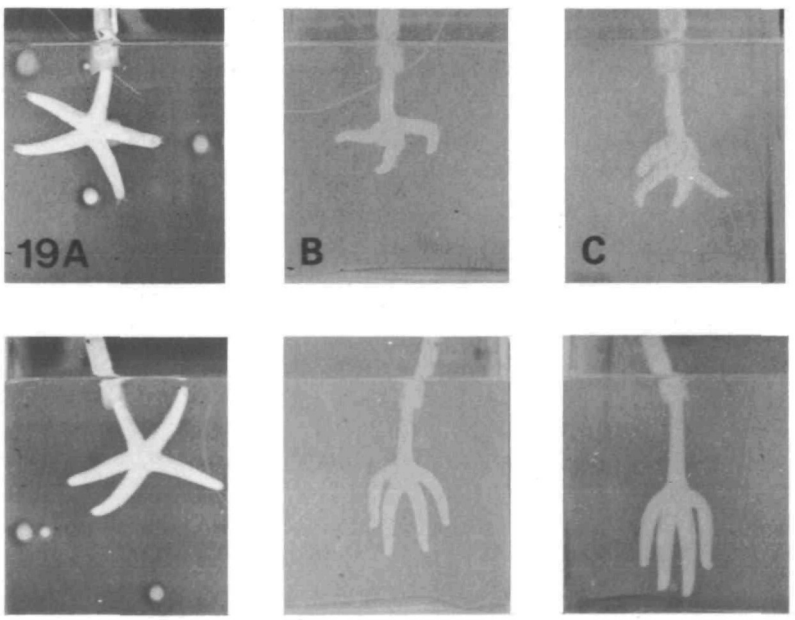

Fig. 19. Effects of anaesthesia on body wall plasticity. Top row: control animal, suspended in aerated artificial sea water. Bottom row: experimental animal, suspended in aerated artificial sea water containing 0.1 % MS222. (A) t=0 min, (B) t=80 min, (C) t=420 min.

friction between the rigid elements and/or strong binding of the joints by powerful tensile elements. Since in *Echinaster* the reticular muscles are tiny, and the ossicles neither interlock geometrically nor actually touch one another, such a framework is unlikely to be particularly strong or rigid. Perhaps the reticular muscles are used to realign ossicles after stress relaxation or large deformations in the body wall. A similar function was suggested for the fine muscle fibrils within the sea urchin spine ligament (Smith *et al.* 1981). The superficial muscle layers of *Echinaster* differ from the expected pattern primarily in the distribution of longitudinal muscle. The longitudinal muscle was concentrated in a single apical strip which was responsible for ray flexion. The circular muscle layer cannot have a hydrostatic function, since the ray is not hydrostatically supported and does not change length during locomotion. Excised pieces of unanaesthetized dorsal body wall would curl tightly after several minutes, indicating powerful contraction of the circular muscles. In the intact ray, this action would produce widening of the ambulacral groove. The circular muscles may also produce ray torsion by asymmetrical contraction. Both longitudinal and circular muscles may be involved in restoring body wall dimensions after the large deformations that occur during righting and hyperextension.

The thick dermal collagen layers of *Echinaster* are organized in a three-dimensional array. Previously, the collagen of starfish was described as a feltwork, i.e. a random fibre orientation (Hyman, 1955). This appearance was probably an artefact of the conventional histological techniques employed, which greatly distort connective tissue. The connective tissue in sections of the *Echinaster* dermis, when subjected to conventional histology, also showed little organization. Even in polarized light, most of the birefringence was lost and no pattern was evident in fixed, decalcified, stained sections. Frozen sections revealed collagen fibres most distinctly. It would not be surprising if other starfish have highly organized collagenous networks, but these may not have been observed owing to inappropriate preparation.

Orthogonal fibre arrays deliver excellent dimensional stability, as manufacturers of fabrics (Gordon, 1978) and radial belted tyres are well aware (Colechin, 1984). Random arrays, in contrast, are generally quite extensible and best suited for loading situations in which the direction of the stress is unpredictable. Since the movements of starfish are highly stereotyped and the stresses on the body wall are predictable, a more ordered fibre network is advantageous. It must be emphasized, however, that the orthogonal collagen network of *Echinaster* is not as neatly organized as woven fabric or the orientated collagen arrays reported for some types of skin (e.g. sharks, Wainwright *et al.* 1978, or eels, Hebrank, 1980). Fibres do change direction as they join other fibre bundles; this interweaving prevents delamination and distributes loads throughout the network.

The interaction between orthogonal fibres and the ossicles is complex and is best understood by examining models that add elements in stages (Fig. 20). At small extensions, orthogonal networks, like fabrics, are usually less stiff on the bia (Wainwright, 1982), since the spaces between the fibres collapse as the fibres align

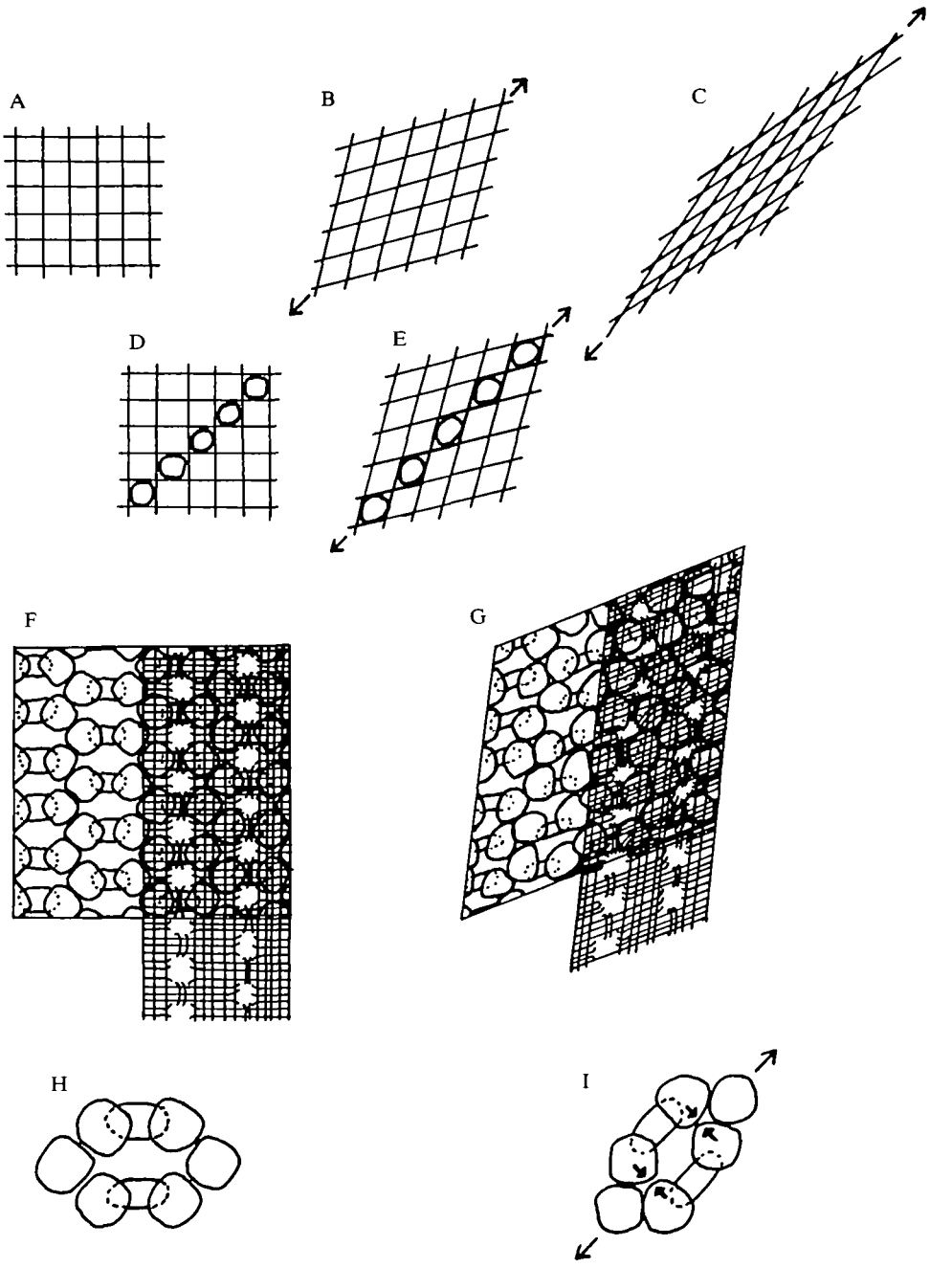

Fig. 20. Bias loading in orthogonal fibre arrays, and the interaction of fibres and rigid elements (see text). (A–C) Orthogonal array. (D–E) Orthogonal array containing rigid elements in some voids. (F) Schematic representation of *Echinaster spinulosus* dermis; left portion shows ossicles, bottom portion shows collagen fibre array, upper right portion shows overlay of both. (G) *E. spinulosus* dermis pulled on the bias. (H) Isolated ossicle ring. (I) Ossicle ring deformed on bias, showing interference of ossicles (arrows).

with the stress (Fig. 20A,B). At large extensions, however, the meshwork collapses entirely, both 'warp' and 'weft' fibres run parallel to the stress, and the fabric acts as a parallel-fibred material in tension (Fig. 20C). It is stiffer and stronger than it was when pulled in the longitudinal or transverse directions. The addition of rigid bodies to the models further modifies the properties (Fig. 20D,E). The rigid bodies sit freely in the voids and are not attached directly to the fibres, mimicking the interaction of the elements of the ossicle layer. In longitudinal or transverse tension, the rigid bodies have essentially no effect, because the load is borne by the fibres parallel to the applied force. In bias loading, the voids begin to collapse but are prevented from complete collapse by the rigid bodies (Fig. 20E). Once the fibre lattice has deformed to this point, both longitudinal and transverse fibres bear the load, as in Fig. 20C. However, owing to the rigid elements, the material becomes even stiffer on the bias once the initial deformation is accomplished. This is why *Echinaster* dorsal body wall is stiffer on the bias after an initial low-modulus phase. In the model material, all tensile stresses are borne by the fibres; the rigid bodies are squeezed by the fibres and are loaded only in compression. A version of this stress distribution occurs within the ossicle layer. Although small collagen fibres are attached to the ossicles, which are therefore not immune to tensile stress, the large load-bearing fibres detour around the ossicles and do not insert directly into them. The large fibres were usually stripped away from the envelope of smaller fibres which surrounded the ossicle. The cracks within the ossicle were probably produced by compression by the large (load-bearing) fibres as the fibre lattice contracted. If the cracks had been produced by tensile failure of the ossicles, the ossicle fragments would have been pulled apart at the crack and the large fibres would have remained attached to the smaller ones forming the insertion. Therefore, it seems reasonable to conclude that the ossicles are receiving primarily compressive stresses.

The fibres of the inner dermis allow the ossicles to accept an additional source of compressive loading when the larger papular voids collapse (Fig. 20F,G). The papular voids coincide with the centres of the ossicle rings (Fig. 20H). The inner dermal fibres overlie the ossicle rings, leaving the papular void clear (Fig. 20F). When the body wall is pulled on the bias, the papular voids deform (Fig. 20G). The fibres do not limit the deformation, but the ossicles do. As an ossicle ring deforms, the ossicles in the corner positions collide (Fig. 20I), preventing total collapse of the void. This limitation of movement has three consequences: the corner ossicles are loaded in compression, the papular voids remain partially open (preserving respiratory function), and the body wall becomes stiffer and stronger after an initial lower-modulus phase. These analyses show that the material properties, structural arrangements and deformations of the fibrous and rigid elements of the dorsal body wall deliver dimensional stability with flexibility in shear.

The orthogonal array of collagen fibres in the *Echinaster* dermis is probably not unique, as this arrangement would be suitable in other asteroids with fairly rig[illegible] arms. In the holothuroid *Thyone briareus*, Menton and Eisen (1970) described an

orthogonal array of thick collagenous lamellae in the dermis. Micrographs of a helical collagen array from holothurian dermis were published by Elder (1973), although Motokawa (1982*a*) reported that holothurian dermis contained a random feltwork of collagen fibres. Fibre arrays previously described in the skin and body wall of other organisms are generally helically arranged (Clark and Cowey, 1958; Gosline, 1971; Harris and Crofton, 1957; Hebrank, 1980; Wainwright *et al.* 1976, 1978; Ward, 1972; Ward and Wainwright, 1972). However, these helical arrays are typical of organisms whose body cavities are pressurized. The crossed helical fibres allow the organism to change length and diameter, bend without buckling, and resist torsion (Wainwright, 1982, 1988). The coelomic cavity of *Echinaster* is not pressurized, nor do the rays change dimension during normal walking. When the starfish bends the ray laterally, the dorsal body wall on the side undergoing compression does indeed buckle. Likewise, during flexion, the dorsal body wall buckles in the area of greatest curvature. In hyperextension, buckling of the ventral body wall does not usually occur since the ambulacral groove can change dimension. Buckling does not imply that *Echinaster* is poorly designed; rather, it seems that local buckling does not present much of a problem to the animal. Although local buckles mechnically represent stress concentrations, the body wall of *Echinaster* is fairly tough, so that cracking is unlikely. The fibres simply slacken, like wrinkles in cloth. Moreover, there are no blood vessels, large nerves or other important conduits within the dorsal body wall to be pinched off when buckling occurs. Once buckling has occurred, it can take several minutes for the creases to flatten out after the ray has straightened. During this time, the animal suffers no apparent ill effects, such as surface cracks, loss of mobility, etc. For *Echinaster*, the dimensional stability conferred by an orthogonal network apparently outweighs any disadvantages caused by buckling.

One important property of the orthogonal fibre array wrapped around a cylinder is its ability to undergo torsion. Torsion is generally avoided both by engineers and in natural selection because it generates very large stresses on the surface of the twisted member when even moderate forces are applied (Gordon, 1978; Higdon *et al.* 1976). However, *Echinaster* and other slender-rayed starfish routinely use torsion in the process of righting (P. O'Neill, personal observation). Torsion of a ray is a manoeuvre which can be accomplished in extremely limited space. An *Echinaster* 1 cm thick can right itself by this method in a cavity less than 2 cm high or in 2 cm of water without exposing any of its body to the air. Methods of righting used by other asteroids, such as the 'tulip' method or body rolling (Reese, 1966), cannot be accomplished in such limited spaces. Manoeuvrability in limited spaces is an important advantage for organisms in habitats such as rocky rubble, oyster beds or shallow water.

The orthogonal fibre array is ideal for torsion, since the voids can collapse as the dorsal body wall is loaded on the bias (shear). Once the voids have collapsed, the body wall then becomes a stiff and strong material which can withstand the stress as the rest of the body is pulled over (P. O'Neill, in preparation).

It is difficult to compare the properties of the dorsal body wall and other

Table 3. *Comparison of mechanical properties of starfish and mammalian tissues*

Tissue	E (MPa)	Breaking stress (MPa)	Breaking strain (%)
Starfish dorsal body wall	249–353	37–45	12–15
Cat skin*	0.30–5.5	12	206
Rat tail tendon†	1304	40–80	5–17

* Veronda and Westmann (1970); strain rate approx. 6 % min^{-1}.
† Kastelic and Baer (1980); strain rate 8 % min^{-1}.

collagenous structures, since the body wall is in reality a complex composite material. The tissue which most resembles the asteroid body wall would be holothuroid dermis, the Young's modulus of which was estimated by Motokawa (1984*a*) from the linear portion of stress–strain curves. E was 1.67 MPa for a 'stiff' species, *Actinopyga echinites*, and 0.42 MPa for a 'soft' species, *Holothuria leucospilota*. Thus E of the *Echinaster* dorsal body wall is two orders of magnitude greater. To give a broader comparison, the *Echinaster* dorsal body wall can be contrasted with mammalian tendon, in which the collagen fibres are all parallel to the principal stress, and mammalian skin, in which the fibres form a random feltwork (Table 3). The dorsal body wall is about an order of magnitude less stiff than tendon, although it has about the same strength. The extensibility is similar to tendon from juvenile rats. Compared with skin, the dorsal body wall is substantially stiffer and 3–4 times as strong, but skin is much more extensible. Compared with other collagenous connective tissues, *Echinaster* dorsal body wall is fairly stiff and strong in its static properties. The high Young's modulus and ultimate tensile strength indicate that the collagen fibres act as continuous elements.

To make a different type of comparison with other collagenous tissues, a mathematical model of a tissue was developed using the architecture of the dorsal body wall as a guide. The model posed the following question. What would the E value of a tissue like the dorsal body wall be if it were constructed of mammalian connective tissue? The model tissue used mammalian tendon, with $E=1$ GPa, as a starting point. The fibres were then oriented orthogonally, so that 50 % were parallel to the applied stress and 50 % were perpendicular. Changing fibre orientation has no effect on the contribution of the matrix component to stiffness, based on the 'rule of mixtures' (Harris, 1980):

$$E_c = \eta E_f V_f + E_m(1-V_f),$$

where c, f and m refer to the composite, fibres and matrix, respectively, V is the volume fraction, and η is Krenchel's efficiency factor (Krenchel, 1964). Krenchel's η is calculated as:

$$\eta = \Sigma \alpha_n \cos^4 \phi,$$

where α is the proportion of the fibres lying along a particular axis and ϕ is the angle the fibres make with the applied stress (Krenchel, 1964). For an orthogonal array, $\eta=0.5$. Therefore, the modulus of an orthogonal fibre network would be half that of a parallel-fibred network, all other factors being equal, and the modulus of the model tissue drops from 1 GPa to 500 MPa.

Next, 10 % voids were added to the model tissue. The effect of voids was modelled using Nielsen's (1967) modification of Kerner's (1956) equation:

$$\frac{1}{E_c}=\frac{1}{E_m}\left\{1+\frac{V_m}{V_f}\left[\frac{15(1-\nu_m)}{7-5\nu_m}\right]\right\},$$

where ν_m is Poisson's ratio for the matrix phase. The ν of collagen was estimated as 0.5 (Wainwright *et al.* 1976). In this case, the 'matrix' was the orthogonal model tissue and the 'fillers' were voids. The presence of 10 % voids ($V_f=0.10$, $V_m=0.90$) reduced the modulus of the model tissue from 500 to 422 MPa.

Finally, 30 % rigid spherical fillers were added to mimic the effect of the ossicles. Nielsen's (1967) version of Kerner's (1956) equation for rigid spheres is:

$$E_c=E_m\left\{1+\frac{V_f}{V_m}\left[\frac{15(1-\nu_m)}{8-10\nu_m}\right]\right\}.$$

Corrections for apparent volume *vs* true volume of the filler (Mooney, 1951) were not used since the true volume had been determined directly from histological preparations of the dorsal body wall. The effect of the filler was to increase E of the model from 422 to 874 MPa.

The model tissue would be somewhat stiffer than the actual dorsal body wall ($E\approx300$ MPa). The disparity is most probably caused by overestimation of the effect of the rigid filler. Filler theories are accurate only for very small particles (around 100 μm in diameter) and are sensitive to the surface area of the filler particles. An ossicle has an external surface area which is orders of magnitude less than the equivalent volume of small particles. Obviously, the ossicles are not acting in the same way as fillers. Nevertheless, the modulus of the model tissue is close enough to that of the dorsal body wall to be able to conclude that the elastic modulus of starfish collagen is not markedly different from that of mammalian tendon collagen.

The high-modulus, continuous-fibre state discussed above probably reflects the properties of the body wall when the connective tissue is in the catch state. The data were derived from tissues excised from starfish which had been handled until they were stiff, which ought to induce catch in the connective tissue, as it does in echinoid spine ligaments (Smith *et al.* 1981). The properties of the connective tissue undergo a fundamental transformation during stress relaxation, however.

The process of stress relaxation allows the dorsal body wall to soften. Large strains are accomplished only during long-term loading. The τ spectrum allows the delineation of 'long-term' and 'short-term' phenomena on the time scale of the starfish. Short-term loading would include any load applied or sustained for less

than 10 s; long-term loading would refer to any load applied or sustained for more than 1000 s. Between these extremes, the body wall is pliant and leathery.

Stress relaxation in the dorsal body wall was slightly anisotropic, since longitudinal stress relaxed slightly faster than stresses in the other test directions. τ_{max} for the longitudinal direction was 2.96 (=912 s or about 15 min); for the transverse direction, τ_{max} was 3.35 (=2239 s or about 37 min); and for the bias direction, τ_{max} was 3.32 (=2089 s or about 35 min). The spectra are all similarly asymmetrical, revealing that stress relaxation was slow at first, gradually increased to the τ peak, then proceeded extremely rapidly. After about 4.5 h, the stress decayed to very low levels and the dorsal body wall was plastically deformed.

It is possible that muscle contraction in the unanaesthetized tissue strips (Fig. 17A) influenced the course of stress relaxation in these experiments. The difference between the curves from unanaesthetized and anaesthetized tissues, although very slight, may have been due to muscular forces competing with stress relaxation, although other independent processes cannot be ruled out.

The relaxation times for *Echinaster* dorsal body wall are greater than those for holothuroid dermis tested in artifical sea water (Motokawa, 1984*a*). Motokawa used two different methods of determining τ. In the first, τ was estimated as the time at which the initial stress fell to 1/e of its initial value, which gave τ=8.03 s for *Actinopyga* and τ=15.3 s for *Holothuria*. His more precise method involved modelling the dermis as two parallel Maxwell elements, which yielded two relaxation times for the dermis of each species: 12 and 160 s for *Actinopyga* and 1.7 and 82 s for *Holothuria*. The methods used in this paper for determination of a τ spectrum are not strictly equivalent to Motokawa's, since the Alfrey approximation assumes that the material behaves like an infinite number of Maxwell elements instead of only two. In addition, Motokawa did not anaesthetize the tissues. The differences in the discrete τ values reported by Motokawa and the peaks of the τ spectra in this study, however, are large enough to conclude that the *Echinaster* connective tissue is either more cross-linked or more collagenous than holothuroid dermis. Motokawa's data showed that most of the stress relaxation events in the holothuroid dermis were over after 200 s; in *Echinaster* the main stress relaxation was just beginning at this time.

The stress relaxation curves indicated that the connective tissue contains a labile cross-link which was broken during stress relaxation. Since the τ spectrum was so broad, there may have been several similar cross-links which were being altered during stress relaxation. The fracture surfaces of the stress-relaxed tissue showed that the large fibres dissociated and that smaller fibrils shredded away from them. This type of fracture never occurred in unrelaxed tissue. The low tensile strength of stress-relaxed tissue also indicated that a break in the continuity of the fibres had occurred. Therefore, a labile cross-link is implicated in binding the small fibrils into the larger fibres. Once the small fibrils were released, they sheared through the proteoglycan matrix. *Echinaster* connective tissue that dissociated during stress relaxation resembled connective tissue from other echinoderms th[illegible] had undergone autotomy: dispersed fibres in holothuroid introvert (Byrne,

1985*a*), bent and tangled broken fibrils in crinoid ligaments (Holland and Grimmer, 1981), and the 'disoriented swirl of fibres' in which 'collagen fibrils are loosened and spread out, as if the means by which cohesion is normally maintained within the ligament had been lost' in ophiuroid ligaments (Wilkie, 1978*a*).

It is interesting that the stress relaxation process in *E. spinulosus* bears some resemblance to the ion-induced softening which occurs in other echinoderm tissues (see Wilkie, 1984, for a review). Both processes involve a decrease in modulus and dissociation of fibrils, but stress relaxation is much slower than variable tensility. Ions are known to enhance or retard the rate of stress relaxation (or its converse, creep) in echinoderm connective tissues examined thus far (Byrne, 1985*a*; Eylers, 1982; Greenberg and Eylers, 1984; Motokawa, 1984*a*; Motokawa and Hayashi, 1987). Are ions acting as modifiers of the basic viscoelastic properties of echinoderm connective tissue (i.e. affecting the same cross-links), or are they initiating a totally separate process (i.e. affecting different cross-links)? Existing studies, including this one, cannot distinguish between these alternatives, which surely merit further study.

Is it possible for an echinoderm to rely solely on viscoelastic processes without recourse to ionic manipulation of the connective tissue? The behavioural, morphological and viscoelastic parameters presented in this study can shed some light on this question. *Echinaster* could exploit the viscoelastic behaviour of its body wall by applying small muscular forces to it for relatively long periods, by moving slowly, or by allowing the body wall to deform under its own weight or the weight of a ray. For example, a 50 % decrease in modulus can be obtained in the longitudinal direction by loading the body wall for about 6 min. Some simple calculations can show, however, that stress relaxation alone cannot be the only process exploited by *Echinaster* when the body wall undergoes large strains. Ray hyperextension is one movement that is easy to analyse in terms of known loads on the dorsal body wall and musculature involved. In hyperextension, the dorsal body wall is strained to a maximum of 10–13 % in the longitudinal direction. This movement would generate a stress of 27 MPa, based on the static E (presumably from tissue in catch) and a 10 % strain. The maximum strain occurs along the centre strip of the ray, a region about 1 mm wide and 1 mm thick. Therefore, a force of 27 N would be required to stretch the strip to 10 % strain. The muscles responsible for hyperextension are the longitudinal adambulacral muscles (located in pairs on each side of the ray between the adambulacral ossicles with a cross-section of 1 mm^2 each) and the longitudinal ambulacral muscles (located in pairs between the ambulacral ossicles with a cross-section of 0.5 mm^2 each). If these muscles were capable of generating tensions equivalent to the *Mytilus* anterior byssus retractor muscle (the strongest known invertebrate smooth muscle, Cole and Twarog, 1972), they could produce a total of 4.5 N. This is not enough tension to hyperextend the tissue strip, let alone the rest of the dorsal surface of the ray. Hyperextension takes about 30 s to occur (Table 1) once the starfish begins to move. If the dorsal body wall were to stress-relax for this period, the longitudinal E would drop to 83 % of its initial value and the power requirement would fall to

22 N. This value is still too high. For the power requirement to fall into a biologically realistic range, the starfish would have to take about 42 min to hyperextend the arm, so that E would drop by an order of magnitude. *Echinaster* is slow, but it isn't that slow. Similar calculations can be made for other ray movements, but the results are comparable. The force required for the strain and the maximum tension that the muscles could generate are mismatched by about an order of magnitude.

The body wall must therefore be in a more pliant state for movements involving significant tensile strains. Behavioural observations bear this out. If an animal is involved in ray flexion, hyperextension, lateral bending or torsion, and is rapidly seized, the body wall clearly feels soft. Within 15–20 s, it stiffens. When an animal is walking about or resting on a vertical surface, it feels quite firm. Therefore, walking and resting probably involve the catch state of the connective tissue.

Echinaster may need to use ionic manipulation of the proteoglycan matrix of the collagen to modify the modulus of the body wall for other movements. The precise role of ions in affecting the τ spectrum in asteroids is currently under investigation. However, the experiments with anaesthetized whole animals proved that a functioning nervous system was necessary to maintain body wall stiffness; otherwise, the animal would melt every time it remained still for more than a few minutes. Rapid changes in the stiffness of the body wall, such as those that occur during autotomy, are most likely to involve ionic manipulation. These changes are under nervous control (Wilkie, 1978*a*). Aside from autotomy, it has not been definitively demonstrated whether ionically induced changes in the modulus of collagenous tissues of other echinoderms are routinely used for normal movements *in vivo*, although Motokawa (1984*a*) pointed out numerous instances where this probably occurs. Ion pumps, after all, require energy for active transport, and it has been demonstrated that echinoderms have very low metabolic rates (La Barbera, 1982; Webster, 1975; Miller *et al.* 1971). Stress relaxation may interact synergistically with ionic processes. The data presented in this study indicate that mutable behaviour of the connective tissue would probably be necessary for most of the ray movements of *Echinaster*, but not for normal walking or resting. Whether other echinoderms fit this pattern is unknown.

The structure and mechanical properties of the body wall of *Echinaster* impose certain limits on its niche. Since any movements that require large strains in the body wall must be made slowly to allow for stress relaxation and/or ionic changes, only slow moving or stationary prey are suitable. However, since asteroids have low energetic requirements (Webster, 1975; Miller *et al.* 1971), they can exploit habitats in which food is highly irregular in its temporal distribution, and the animals can tolerate long periods of starvation. The flexibility of the body wall allows the starfish to utilize habitats which contain shallow water and small crevices; such habitats are unavailable to similarly sized animals with more rigid body walls. In addition, the body wall confers stiff, strong protection if it is rapidly loaded, whether by waves, rock impacts or the jaws and claws of predator[redacted] Ultimately, ion-sensitive connective tissue may restrict the echinoderms to marine

environments, as Eylers (1982) has suggested. Thus, the mechanical properties of the body wall present the animal with a set of opportunities and constraints which help to determine its niche.

This study was supported by research funding and a postdoctoral fellowship to the author from the Cocos Foundation, Inc.; additional funding was provided by the Portland State University, N.I.H. Biomedical Research Support Programme, and the University of Western Australia 75th Anniversary Re-entry Postdoctoral Research Fellowship.

References

ALFREY, T. AND DOTY, P. (1945). The methods of specifying the properties of viscoelastic materials. *J. appl. Physics* **16**, 700–713.

ARMSTRONG, S. A. (1987). Mechanical properties of the tissues of the brown alga *Hedophyllum sessile* (C.Ag) Setchell: variability with habitat. *J. exp. mar. Biol. Ecol.* **114**, 143–151.

BYRNE, M. (1985*a*). The mechanical properties of the autotomy tissues of the holothurian *Eupentacta quinquesemita* and the effect of certain physico-chemical agents. *J. exp. Biol.* **117**, 69–86.

BYRNE, M. (1985*b*). Ultrastructural changes in the autotomy tissues of *Eupentacta quinquesemita* (Selenka) (Echinodermata: Holothuroidea) during evisceration. In *Echinodermata* (ed. B. F. Keegan and B. D. S. O'Connor), pp. 413–420. Rotterdam: A. A. Balkema.

CHRISTENSEN, A. M. (1957). The feeding behavior of the seastar *Evasterias troschelli* Stimpson. *Limnol. Oceanogr.* **2**, 180–197.

CLARK, R. D. AND COWEY, J. B. (1958). Factors controlling the change of shape of certain nemertean and turbellarian worms. *J. exp. Biol.* **35**, 731–748.

COLE, R. A. AND TWAROG, B. M. (1972). Relaxation in a molluscan smooth muscle. I. Effects of drugs which act on the adenyl cyclase system. *Comp. Biochem. Physiol.* **43**A, 321–330.

COLECHIN, L. (1984). *Motor Vehicles: Vehicle Wheels and Tyres.* Canberra: Aust. Govt Pub. Service.

CURREY, J. D. (1975). A comparison of the strength of echinoderm spines and mollusc shells. *J. mar. Biol. Ass. U.K.* **55**, 419–424.

DENNY, M. W., DANIEL, T. L. AND KOEHL, M. A. R. (1985). Mechanical limits to size in wave-swept organisms. *Ecol. Monogr.* **55**, 69–102.

DORRINGTON, K. L. (1980). The theory of viscoelasticity in biomaterials. In *Mechanical Properties of Biological Materials* (ed. J. F. V. Vincent and J. D. Currey), pp. 290–314. Cambridge: Cambridge University Press.

ELDER, H. Y. (1973). Distribution and function of elastic fibres in the invertebrates. *Biol. Bull. mar. biol. Lab., Woods Hole* **144**, 43–63.

EYLERS, J. P. (1976). Aspects of skeletal mechanics of the starfish *Asterias forbesii*. *J. Morph.* **149**, 353–368.

EYLERS, J. P. (1982). Ion-dependent viscosity of holothurian body wall and its implications for the functional morphology of echinoderms. *J. exp. Biol.* **99**, 1–8.

GORDON, J. E. (1978). *Structures, or Why Things Don't Fall Down.* Harmondsworth: Penguin Books Ltd.

GOSLINE, J. M. (1971). Connective tissue mechanics of *Metridium senile*. II. Visco-elastic properties and macromolecular model. *J. exp. Biol.* **55**, 775–795.

GREENBERG, A. R. AND EYLERS, J. P. (1984). Influence of ionic environment on the stress relaxation behaviour of an invertebrate connective tissue. *J. Biomech.* **17**, 161–166.

GURR, E. (1962). *Staining Animal Tissue – Practical and Theoretical.* London: Leonard Books Ltd.

HAROLD, A. S. (1985). Body wall structure of *Echinarachnius parma* (Echinoidea:

Clypeasteroidea). In *Echinodermata* (ed. B. F. Keegan and B. D. S. O'Connor), p. 388. Rotterdam: A. A. Balkema.

HARRIS, B. (1980). The mechanical behaviour of composite materials. In *Mechanical Properties of Biological Materials* (ed. J. F. V. Vincent and J. D. Currey), pp. 37–74. Cambridge: Cambridge University Press.

HARRIS, J. E. AND CROFTON, H. D. (1957). Structure and function in the nematodes: internal pressure and cuticular structure in *Ascaris*. *J. exp. Biol.* **34**, 116–130.

HEBRANK, M. R. (1980). Mechanical properties and locomotor functions of eel skin. *Biol. Bull. mar. biol. Lab., Woods Hole* **158**, 58–68.

HIDAKA, M. (1983). Effects of certain physico-chemical agents on the mechanical properties of the catch apparatus of the sea-urchin spine. *J. exp. Biol.* **103**, 15–29.

HIGDON, A., OHLSEN, E. H., STILES, W. B., WEESE, J. A. AND RILEY, W. F. (1976). *Mechanics of Materials*, third edn. New York: John Wiley & Sons.

HOLLAND, N. D. AND GRIMMER, J. C. (1981). Fine structure of syzygial articulations before and after arm autotonomy in *Florometra serratissima* (Echinodermata: Crinoidea). *Zoomorph.* **98**, 169–183.

HYMAN, L. H. (1955). *The Invertebrates: Echinodermata.* New York: McGraw-Hill.

KASTELIC, J. AND BAER, E. (1980). Deformation in tendon collagen. In *Mechanical Properties of Biological Materials* (ed. J. F. V. Vincent and J. D. Currey), pp. 397–435. Cambridge: Cambridge University Press.

KERKUT, G. A. (1955). The retraction and protraction of the tube feet of the starfish (*Asterias rubens* L.). *Behavior* **8**, 112–129.

KERNER, E. H. (1956). The elastic and thermo-elastic properties of composite media. *Proc. Phys. Soc.* **69B**, 808–813.

KOEHL, M. A. R. (1977). Mechanical diversity of connective tissue of the body wall of sea anemones. *J. exp. Biol.* **69**, 107–125.

KOEHL, M. A. R. (1982). Mechanical design of spicule-reinforced connective tissue: stiffness. *J. exp. Biol.* **98**, 239–267.

KOEHL, M. A. R. (1984). How do benthic organisms withstand moving water? *Am. Zool.* **24**, 57–70.

KOEHL, M. A. R. AND WAINWRIGHT, S. A. (1977). Mechanical adaptations of a giant kelp. *Limnol. Oceanogr.* **22**, 1067–1071.

KRENCHEL, H. (1964). *Fibre Reinforcement.* Copenhagen: Akodemisk Forlag.

LA BARBERA, M. (1982). Metabolic rates of suspension feeding crinoids and ophiuroids (Echinodermata) in a unidirectional laminar flow. *Comp. Biochem. Physiol.* **71A**, 303–307.

LANIR, Y., WALSH, J. AND SOUTAS-LITTLE, R. W. (1984). Histological staining as a measure of stress collagen fibres. *J. Biomech. Engr.* **106**, 174–176.

MENTON, D. N. & EISEN, A. Z. (1970). The structure of the integument of the sea cucumber, *Thyone briareus*. *J. Morph.* **131**, 17–36.

MILLER, R. J., MANN, K. H. AND SCARRATT, D. J. (1971). Production potential of a seaweed–lobster community in eastern Canada. *J. Fish. Res. Bd Can.* **28**, 1733–1738.

MOONEY, M. (1951). The viscosity of a concentrated suspension of spherical particles. *J. Colloid Sci.* **6**, 162–170.

MOTOKAWA, T. (1981). The stiffness change of the holothurian dermis caused by chemical and electrical stimulation. *Comp. Biochem. Physiol.* **70C**, 41–48.

MOTOKAWA, T. (1982*a*). Fine structure of the dermis of the body wall of the sea cucumber, *Stichopus chloronotus*, a connective tissue which changes its mechanical properties. *Galaxea* **1**, 55–64.

MOTOKAWA, T. (1982*b*). Rapid change in mechanical properties of echinoderm connective tissues caused by coelomic fluid. *Comp. Biochem. Physiol.* **73C**, 223–229.

MOTOKAWA, T. (1984*a*). Viscoelasticity of holothurian body wall. *J. exp. Biol.* **109**, 63–75.

MOTOKAWA, T. (1984*b*). Connective tissue catch in echinoderms. *Biol. Rev.* **59**, 255–270.

MOTOKAWA, T. AND HAYASHI, Y. (1987). Calcium dependence of viscosity change caused by cations in holothurian catch connective tissue. *Comp. Biochem. Physiol.* **87A**, 579–582.

NIELSEN, L. E. (1967). Mechanical properties of particulate-filled systems. *J. Compos. Materials* **1**, 100–119.

PUTT, F. A. (1972). *Manual of Histopathological Staining Methods*. New York: John Wiley & Sons.

REESE, E. S. (1966). The complex behavior of echinoderms. *In Physiology of Echinodermata* (ed. R. A. Boolootian), pp. 157–218. New York: Wiley Interscience.

SCHEIBLING, R. E. (1982). Differences in body size and growth rate between morphs of *Echinaster* (Echinodermata: Asteroidea) from the eastern Gulf of Mexico. In *Echinoderms: Proceedings of the International Conference Tampa Bay* (ed. J. M. Lawrence), pp. 291–298. Rotterdam: A. A. Balkema.

SMITH, D. S., WAINWRIGHT, S. A., BAKER, J. AND CAYER, M. L. (1981). Structural features associated with movement and "catch" of sea-urchin spines. *Tissue & Cell* **13**, 299–320.

TELFORD, M. (1985). Structural analysis of the test of *Echinocyamus pusillus* (O. F. Müller). In *Echinodermata* (ed. B. F. Keegan and B. D. S. O'Connor), pp. 353–359. Rotterdam: A. A. Balkema.

VERONDA, D. R. AND WESTMANN, R. A. (1970). Mechanical deformation of skin – finite deformations. *J. Biomechanics* **3**, 111–124.

VOGEL, S. (1981). *Life in Moving Fluids: The Physical Biology of Flow*. Boston: Willard Grant Press.

VOGEL, S. (1984). Drag and flexibility in sessile organisms. *Am. Zool.* **24**, 37–44.

WAINWRIGHT, S. A. (1982). Structural systems: hydrostats and frameworks. In *A Companion to Animal Physiology* (ed. C. R. Taylor, K. Johansen and L. Bolis), pp. 325–338. Cambridge: Cambridge University Press.

WAINWRIGHT, S. A. (1988). *Axis and Circumference. The Cylindrical Shape of Plants and Animals*. Cambridge, MA: Harvard University Press.

WAINWRIGHT, S. A., BIGGS, W. D., CURREY, J. D. AND GOSLINE, J. M. (1976). *Mechanical Design in Organisms*. New York: John Wiley & Sons.

WAINWRIGHT, S. A., VOSBURGH, F. AND HEBRANK, J. H. (1978). Shark skin: function in locomotion. *Science* **202**, 747–749.

WARD, D. V. (1972). Locomotor function of the squid mantle. *J. Zool., Lond.* **167**, 487–499.

WARD, D. V AND WAINWRIGHT, S. A. (1972). Locomotor aspect of squid mantle structure. *J. Zool., Lond.* **167**, 487–499.

WEBSTER, S. K. (1975). Oxygen consumption in echinoderms from several geographic locations, with particular reference to the Echinoidea. *Biol. Bull. mar. biol. Lab., Woods Hole* **148**, 165–180.

WELLS, K. F. (1966). *Kinesiology*, 4th edn. Philadelphia: W. B. Saunders Co.

WILKIE, I. C. (1978*a*). Arm autotomy in brittlestars (Echinodermata: Ophiuroidea). *J. Zool., Lond.* **186**, 311–330.

WILKIE, I. C. (1978*b*). Nervously mediated change in the mechanical properties of a brittlestar ligament. *Mar. Behav. Physiol.* **5**, 289–306.

WILKIE, I. C. (1983). Nervously mediated change in the mechanical properties of the cirral ligament of a crinoid. *Mar. Behav. Physiol.* **9**, 229–248.

WILKIE, I. C. (1984). Variable tensility in echinoderm collagenous tissues: a review. *Mar. Behav. Physiol.* **11**, 1–34.